Electronic Supplementary Material (ESI) for ChemComm.
This journal is © The Royal Society of Chemistry 2021

Supported permethylindenyl post-metallocene titanium catalysts for the synthesis of disentangled ultra high molecular weight polyethylene (*dis*UHMWPE)

Clement G. Collins Rice, Jean-Charles Buffet, Zoë R. Turner, and Dermot O'Hare

Chemistry Research Laboratory, University of Oxford, 12 Mansfield Road, Oxford, OX1 3TA, U.K.

Table of contents

1. General details and instrumentation

General procedures. Air- and moisture-sensitive compounds were manipulated under an inert atmosphere of nitrogen, using standard Schlenk line techniques[1] on a dual manifold vacuum/nitrogen line or in an MBraun Labmaster 100 glovebox.

Pentane, hexane, toluene and benzene were dried using an MBraun SPS 800 solvent purification system, stored over a potassium mirror, and degassed under partial vacuum before use. Anhydrous DCM was dried using an MBraun SPS 800 system, stored over pre-activated 3 Å molecular sieves and degassed under partial vacuum before use. Tetrahydrofuran was distilled from sodium/benzophenone, stored over pre-activated 3 Å molecular sieves and degassed under partial vacuum before use.

Deuterated solvents were dried over potassium metal (benzene-d_6, and toluene-d_8) or CaH_2 (chloroform-*d*, pyridine-d_5, and tetrahydrofuran-d_8) and refluxed under reduced pressure, distilled under static vacuum, freeze-pump-thaw degassed three times and stored over pre-activated 3 or 4 Å molecular sieves. Chloroform-*d* was used as supplied for samples which were not air- and moisture-sensitive.

Solution NMR spectroscopy. NMR spectra were recorded on either a Bruker Avance III HD NanoBay NMR (9.4 T, 400.2 MHz), a Bruker Avance III NMR (11.75 T, 499.9 MHz) or a Bruker Avance NMR (11.75 T, 500.3 MHz) with a ^{13}C-detect cryoprobe. Spectra were recorded at 298 K unless otherwise stated and referenced internally to the residual *protio* solvent resonance. Chemical shifts, δ, are reported in parts per million (ppm) relative to tetramethylsilane (δ = 0 ppm). Air-sensitive samples were prepared in a glovebox under an inert atmosphere of nitrogen, using dried deuterated solvents and sealed in 5 mm Young's tap NMR tubes.

Solid-state NMR spectroscopy. Solid-state NMR spectra were recorded by Dr Nicholas Rees (University of Oxford) on a Bruker Avance III HD NanoBay solid-state NMR spectrometer (9.4 T, 399.9 MHz). Samples were spun at the magic angle at spin rates of 10 kHz for ^{13}C and ^{29}Si, and 20 kHz for ^{1}H and ^{27}Al. ^{13}C NMR spectra were referenced to adamantane, ^{27}Al to aluminium nitrate, and ^{29}Si to kaolinite.

X-ray crystallography. Single-crystal X-ray diffraction data collection and structure determination were performed by Dr Zoë R. Turner (University of Oxford). Crystals were mounted on MiTeGen MicroMounts using perfluoropolyether oil and rapidly transferred to a goniometer head on a diffractometer fitted with an Oxford Cryosystems Cryostream open-flow nitrogen cooling device.[2] Data collections were carried out at 150 K on an Oxford Diffraction Supernova diffractometer using mirror-monochromated Cu Kα radiation (λ = 1.54178 Å) and data were processed using CryAlisPro.[3] The structures were solved using direct methods (SIR-92)[4] or a charge flipping algorithm (SUPERFLIP)[5] and refined by full-matrix least-squares using the Win-GX software suite.[6] Molecular bond lengths and angles were calculated, where required, using PLATON.[7] Illustrations of the solid state molecular structures were created using ORTEP.[8] Thermal ellipsoids were shown at 30% probability.

Elemental analysis. Samples were prepared in a glovebox under a nitrogen atmosphere and sealed in glass vials. CHN analyses were carried out in duplicate by Ms Orla McCullough (London Metropolitan University).

Infrared spectroscopy. Fourier-transform infrared (FTIR) spectra were measured using a ThermoScientific Nicolet iS 5 FTIR spectrometer, and either the iD1 Transmission, or germanium iD3 Attenuated Total Reflection accessories. A background spectrum was run prior to the samples and subtracted from the sample spectra. Air-sensitive samples were prepared in a glove box, ground with anhydrous potassium bromide, and pressed into discs.

Scanning electron microscopy. Scanning electron microscopy (SEM) images were collected on a JEOL JSM-6010LV scanning electron microscope. Samples were prepared on carbon tape and coated with platinum using a Quorum Technologies SC7620 sputter coater to reduce charge buildup and improve image quality.

Gel permeation chromatography. Gel permeation chromatography (GPC) was performed by Ms Liv Thobru, Ms Sara Herum, and Ms Rita Jenssen (Norner AS, Norway) on a high temperature gel permeation chromatograph with an IR5 infrared detector (GPC-IR5). Samples were prepared by dissolution in 1,2,4-trichlorobenzene (TCB) containing 300 ppm of 3,5-di-*tert*-buty-4-hydroxytoluene (BHT) at 160 °C for 90 minutes and then filtered with a 10 µm SS filter before being passed through the GPC column. The samples were run under a flow rate of 0.5 mL min^{-1} using TCB containing 300 ppm of BHT as mobile phase with 1 mg mL^{-1} BHT added as a flow rate marker. The GPC column and detector temperature were set at 145 and 160 °C respectively.

Differential scanning calorimetry. Differential scanning calorimetry was performed on a Perkin Elmer DSC 4000 System within a temperature range of 30–180 °C at a rate of 20 K min^{-1}. Polymer samples were sealed in 100 µL aluminium crucibles. An empty crucible was used as a reference, and the DSC was calibrated using indium and zinc.

Literature preparations and commercially supplied materials. 2,3,4,5,6,7-hexamethylindene (SCG Chemicals Co., Ltd.), ^{n}BuLi (1.6 M in hexanes, Sigma Aldrich), 4-methyl-2-*tert*-butylphenol (Sigma Aldrich), 6-bromo-2,4-di-*tert*-butylphenol (Alfa Aesar), and bromine (Sigma Aldrich) were all used as received. $TiCl_4.2THF$ was prepared according to a literature procedure.[9] Et_3N was dried over KOH, distilled under static vacuum and freeze-pump-thaw degassed before use. 2,4-bis(*α*,*α*-dimethylbenzyl)phenol (Sigma Aldrich) was recrystallized from hot ethanol before use. Me_2SiCl_2 (Sigma Aldrich) was dried over pre-activated 3 Å molecular sieves before use. Allyl bromide was washed with $NaHCO_3$ followed by distilled water and dried over $MgSO_4$. The indenyl-PHENICS complex $^{Me2}SB(^{tBu,Me}ArO,Ind)TiCl_2$ (**6**) was synthesised according to a modified literature procedure.[10] Ethylene was supplied by CK Special Gases Ltd, and passed through molecular sieves before use. Solid polymethylaluminoxane (sMAO) was supplied by SGC Chemicals Co., Ltd. (Thailand) as a slurry in toluene which was dried under vacuum before use. MAO was supplied by Chemtura Corporation as a slurry in toluene which was dried under vacuum before use. Silica was supplied by PQ Corporation (USA), and was calcined by Dr. Philip Kenyon (University of Oxford). LDH was synthesised by Miss Katherine Laney (University of Oxford) according to modified literature procedures.[11,12]

2. Experimental details

2.1 Complex synthesis

Substituted phenol, ^{R1R2}ArOH (1 equivalent), was dissolved in dichloromethane in a round-bottomed flask. To this, Br_2 (1 eq.) was added dropwise. The reaction was stirred for 90 minutes, after which the crude mixture was washed with distilled water. The organic portion was dried over $MgSO_4$, filtered, and the solvent removed under vacuum to yield the monobrominated product quantitatively as a thick oil.

The bromophenol ^{Br,R1R2}ArOH and allyl bromide (CH_2CHCH_2Br, 1.5 eq.) were then dissolved in acetone in a round-bottomed flask. This solution was then added dropwise to a 10% aqueous solution of NaOH (1.5 eq.) and stirred for 4 hours. The reaction mixture was neutralised with 5% aqueous H_2SO_4 and the volatiles removed under vacuum. The product, $^{\mathrm{Br,R1R2}}$ArOAllyl, was extracted in toluene, dried over MgSO$_4$ and the solvent removed under vacuum to give the desired product in quantitative yields as off-white solids.

The allylphenol $^{\mathrm{Br,R1R2}}$ArOAllyl was dissolved in toluene in a Schlenk flask. To this was added dropwise at –70 °C 1.3 eq. of ^{n}BuLi solution (1.6 M in hexanes) and the reaction was allowed to warm to –20 °C. This mixture was then dropwise added to a toluene solution of 3 eq. Me$_2$SiCl$_2$ at –20 °C. The reaction was allowed to warm to room temperature and stirred for 18 h. The solid byproducts were removed by filtration, and the volatiles removed under vacuum, leaving the chlorosilyl product, $^{\mathrm{Me2SiCl,R1R2}}$ArOAllyl, as a pale yellow to colourless oil in yields of 60–85%.

This was then combined with 1.1 equivalents of (2,3,4,5,6,7-hexamethyl-1*H*-inden-1-yl)lithium (Ind$^\#$Li) and dissolved in THF at 0 °C. The reaction was allowed to warm to room temperature and stirred for 18 h, after which it was dried under vacuum; the product was extracted in pentane and the solvent removed under vacuum to yield the proligand $^{\mathrm{Me2}}$SB($^{\mathrm{R1R2}}$ArOAllyl,I*)H in 75 % yield.

To a toluene solution of the proligand and 3.5 equivalents of triethylamine cooled to –78 °C, 2.25 eq. of ^{n}BuLi solution (1.6 M in hexanes) was added dropwise. The reaction was allowed to warm to room temperature and stirred for 3–18 h, during which the solution gradually darkens. To this was then added 1.5 eq. of TiCl$_4$.2THF as a slurry in toluene, and the reaction stirred for 18 h during which the solution became dark red. The insoluble materials were removed by filtration and the volatiles were removed from the filtrate under vacuum. The resulting brick-red solid was washed with pentane to afford the titanium dichloro complexes, $^{\mathrm{Me2}}$SB($^{\mathrm{R1R2}}$ArO,I*)TiCl$_2$. Crystals suitable for single-crystal X-ray diffraction were grown from a saturated pentane solution stored at –30 °C.

$^{\mathrm{Me2}}$SB($^{t\mathrm{Bu,Me}}$ArO,I*)TiCl$_2$ (1). 18% yield.

^{1}H NMR (400 MHz, benzene-d_6, 298 K): δ 7.22 (d, $^4J_{\mathrm{H-H}}$ = 1.9 Hz, 1H, *m*Ph**H**), 7.19 (d, $^4J_{\mathrm{H-H}}$ = 2.0 Hz, 1H, *m*Ph**H**), 2.66 (s, 3H, I***Me**), 2.56 (s, 3H, I***Me**), 2.27 (s, 3H, Ph**Me**), 2.14 (s, 3H, I***Me**), 2.03 (s, 3H, I***Me**), 2.02 (s, 3H, I***Me**), 1.98 (s, 3H, I***Me**), 1.46 (s, 9H, C**Me**$_3$), 0.68 (s, 3H, Si**Me**), and 0.66 (s, 3H, Si**Me**) ppm.

^{13}C{^{1}H} NMR (126 MHz, benzene-d_6, 298 K): δ 167.79 (***i***Ph), 144.68 (**I***), 138.03 (**I***), 136.99 (***o***Ph), 136.95 (**I***), 136.51 (**I***), 134.04 (***o'***Ph), 133.98 (***p***Ph), 132.50 (**I***), 131.98 (**I***), 131.37 (***m***Ph), 131.22 (**I***), 131.01 (**I***), 129.04 (***m***Ph), 110.75 (**1**I*),35.12 (**C**Me$_3$), 30.05 (C**Me**$_3$), 21.81 (I***Me**), 21.44 (Ph**Me**), 17.46 (I***Me**), 17.26 (I***Me**), 16.66 (I***Me**), 16.50 (I***Me**), 15.69 (I***Me**), 3.62 (Si**Me**), and 1.49 (Si**Me**) ppm.

$^{\mathrm{Me2}}$SB($^{t\mathrm{Bu2}}$ArO,I*)TiCl$_2$ (2). 29% yield.

^{1}H NMR (400 MHz, benzene-d_6, 298 K): δ 7.58 (d, $^4J_{\mathrm{H-H}}$ = 2.4 Hz, 1H, *m*Ph**H**), 7.56 (d, $^4J_{\mathrm{H-H}}$ = 2.4 Hz, 1H, *m*Ph**H**), 2.65 (s, 3H, I***Me**), 2.55 (s, 3H, I***Me**), 2.12 (s, 3H, I***Me**), 2.05 (s, 3H, I***Me**), 2.02 (s, 3H, I***Me**), 1.96 (s, 3H, I***Me**), 1.50 (s, 9H, C**Me**$_3$), 1.38 (s, 9H, C**Me**$_3$), and 0.72 (s, 6H, Si**Me**) ppm.

^{13}C{^{1}H} NMR (126 MHz, benzene-d_6, 298 K): δ 167.32 (***i***Ph), 146.91 (***o,p***Ph), 144.39 (**I***), 137.60 (**I***), 136.61 (**I***), 136.15 (**I***), 136.10 (***o,p***Ph), 133.14 (***o'***Ph), 132.24 (**I***), 131.61 (**I***), 130.85 (**I***), 130.62 (**I***), 127.07 (***m***Ph), 124.87 (***m***Ph), 110.40 (**1**I*), 35.11 (**C**Me$_3$), 34.61 (**C**Me$_3$), 31.44 (C**Me**$_3$), 29.73 (C**Me**$_3$), 21.37 (I***Me**), 17.11 (I***Me**), 16.88 (I***Me**), 16.29 (I***Me**), 16.12 (I***Me**), 15.47 (I***Me**), 3.35 (Si**Me**), and 1.44 (Si**Me**) ppm.

^{29}Si NMR (79.5 MHz, benzene-d_6, 298 K): δ –12.60 ppm.

CHN analysis (%): Expected C 64.25, H 7.65; observed C 64.57, H 7.86.

To a solution of **2** in benzene-d_6 was added two equivalents of either Me$_3$SiBr or Me$_3$SiI. The mixtures were heated at 80 °C, until conversion was judged to be complete by ^{1}H NMR spectroscopy. The volatiles were removed under vacuum, to yield the desired dihalo complexes in quantitative yields.

$^{\text{Me2}}$SB($^{t\text{Bu2}}$ArO,I*)TiBr$_2$ (3). 6 hours heating at 80 °C.

^{1}H NMR (500 MHz, benzene-d_6, 298 K): δ 7.58 (d, $^4J_{\text{H–H}}$ = 2.4 Hz, 1H, *m*Ph**H**), 7.57 (d, $^4J_{\text{H–H}}$ = 2.1 Hz, 1H, *m*Ph**H**), 2.71 (s, 3H, I***Me**), 2.62 (s, 3H, I***Me**), 2.13 (s, 3H, I***Me**), 2.04 (s, 3H, I***Me**), 2.03 (s, 3H, I***Me**), 1.97 (s, 3H, I***Me**), 1.58 (s, 9H, C**Me**$_3$), 1.38 (s, 9H, C**Me**$_3$), 0.71 (s, 3H, Si**Me**), and 0.70 (s, 3H, Si**Me**) ppm.

^{13}C{^{1}H} NMR (126 MHz, benzene-d_6, 298 K): δ 168.03 (***i***Ph), 147.45 (***o,p***Ph), 144.77 (**I***), 137.87 (**I***), 137.11 (**I***), 136.77 (**I***), 136.47 (***o,p***Ph), 134.18 (***o′***Ph), 133.24 (**I***), 132.54 (**I***), 131.95 (**I***), 131.66 (**I***), 127.53 (***m***Ph), 125.33 (***m***Ph), 112.04 (**1**I*), 35.64 (**C**Me$_3$), 35.01 (**C**Me$_3$), 31.78 (C**Me**$_3$), 30.34 (C**Me**$_3$), 21.72 (I***Me**), 17.69 (I***Me**), 17.55 (I***Me**), 17.26 (I***Me**), 16.74 (I***Me**), 16.11 (I***Me**), 4.58 (Si**Me**), and 1.73 (Si**Me**) ppm.

^{29}Si NMR (79.5 MHz, benzene-d_6, 298 K): δ –12.49 ppm.

$^{\text{Me2}}$SB($^{t\text{Bu2}}$ArO,I*)TiI$_2$ (4). 1.75 hours heating at 80 °C.

^{1}H NMR (500 MHz, benzene-d_6, 298 K): δ 7.60 (d, $^4J_{\text{H–H}}$ = 2.4 Hz, 1H, *m*Ph**H**), 7.55 (d, $^4J_{\text{H–H}}$ = 2.4 Hz, 1H, *m*Ph**H**), 2.80 (s, 3H, I***Me**), 2.76 (s, 3H, I***Me**), 2.10 (s, 3H, I***Me**), 2.04 (s, 3H, I***Me**), 2.03 (s, 3H, I***Me**), 1.94 (s, 3H, I***Me**), 1.70 (s, 9H, C**Me**$_3$), 1.37 (s, 9H, C**Me**$_3$), 0.69 (s, 3H, Si**Me**), and 0.66 (s, 3H, Si**Me**) ppm.

^{13}C{^{1}H} NMR (126 MHz, benzene-d_6, 298 K): δ 168.47 (***i***Ph), 147.57 (***o,p***Ph), 144.65 (**I***), 137.60 (**I***), 137.20 (**I***), 137.01 (**I***), 136.37 (***o,p***Ph), 135.04 (***o′***Ph), 134.29 (**I***), 133.31 (**I***), 132.82 (**I***), 132.26 (**I***), 127.70 (***m***Ph), 125.45 (***m***Ph), 113.12 (**1**I*), 35.91 (**C**Me$_3$), 35.04 (**C**Me$_3$), 31.74 (C**Me**$_3$), 30.88 (C**Me**$_3$), 21.70 (I***Me**), 19.56 (I***Me**), 18.24 (I***Me**), 17.28 (I***Me**), 16.94 (I***Me**), 16.89 (I***Me**), 5.52 (Si**Me**), and 1.91 (Si**Me**) ppm.

^{29}Si NMR (79.5 MHz, benzene-d_6, 298 K): δ –12.50 ppm.

$^{\text{Me2}}$SB($^{(\text{CMe2Ph})2}$ArO,I*)TiCl$_2$ (5). 12% yield.

^{1}H NMR (400 MHz, benzene-d_6, 298 K): δ 7.51 (d, $^4J_{\text{H–H}}$ = 2.4 Hz, 1H, 3,5-C$_6$**H**$_2$), 7.46 (d, $^4J_{\text{H–H}}$ = 2.4 Hz, 1H, 3,5-C$_6$**H**$_2$), 7.37–7.17 (m, 8H, CMe$_2$**Ph**), 7.13–7.07 (m, 1H, CMe$_2$**Ph**), 7.06–7.00 (m, 1H, CMe$_2$**Ph**), 2.62 (s, 3H, I***Me**), 2.42 (s, 3H, I***Me**), 2.09 (s, 3H, I***Me**), 2.00 (s, 3H, I***Me**), 1.98 (s, 3H, I***Me**), 1.90 (s, 3H, I***Me**), 1.73 (s, 6H, C**Me**$_2$Ph), 1.70 (s, 3H, C**Me**$_2$Ph), 1.67 (s, 3H, C**Me**$_2$Ph), 0.60 (s, 3H, Si**Me**), and 0.59 (s, 3H, Si**Me**) ppm.

^{13}C{^{1}H} NMR (126 MHz, benzene-d_6, 298 K): δ 166.74 (**Ar**), 151.09 (**Ar**), 169.81 (**Ar**), 146.72 (**Ar**), 144.62 (**Ar**), 137.54 (**Ar**), 136.74 (**Ar**), 136.51 (**Ar**), 136.28 (**Ar**), 133.84 (6-**C**$_6$H$_2$), 132.43 (**Ar**), 131.65 (**Ar**), 130.97 (**Ar**), 130.74 (**Ar**), 129.83 (3,5-**C**$_6$H$_2$), 128.46 (CMe$_2$**Ph**), 128.35 (CMe$_2$**Ph**), 128.32 (CMe$_2$**Ph**), 128.16 (CMe$_2$**Ph**), 127.97 (CMe$_2$**Ph**), 127.68 (3,5-**C**$_6$H$_2$), 127.13 (CMe$_2$**Ph**), 126.39 (CMe$_2$**Ph**), 126.19 (CMe$_2$**Ph**), 125.58 (CMe$_2$**Ph**), 110.69 (**I***Si), 43.34, and 42.92 (**C**Me$_2$Ph), 31.26, 31.23, 30.60 and 29.00 (C**Me**$_2$Ph), 21.65, 17.44, 17.31, 16.65, 16.39, and 15.66 (I***Me**), 3.93, and 1.41 (Si**Me**) ppm. An additional aromatic resonance was expected by not observed.

CHN analysis (%): Expected C 69.98, H 6.88; observed C 71.33, H 7.65.

2.2 Solid catalyst synthesis and polymerisation

Synthesis of solid catalysts. The quantity of catalyst immobilised on the surface of the support is given in terms of the Al:Ti ratio of the methylaluminoxane (MAO) component to the organometallic complex. In the case of SSMAO and LDHMAO, 40wt% MAO was used to activate the surface of each support. The Al:Ti ratio used in this work is 200:1. SSMAO and LDHMAO are prepared by weighing out silica or LDH and MAO into a Schlenk in a glovebox and then adding toluene (40 mL) to the mixture, heating at 80 °C for 2 h with regular swirling and then drying under vacuum (1×10^{-2} mbar) at room temperature for at least 4 h to ensure all the solvent was removed. The finished solid catalysts were synthesised according to the following method: in a glove box the inorganic support (SSMAO, LDHMAO or sMAO) and the desired complex were weighed into a Schlenk in a $[\mathrm{Al}_{\mathrm{MAO}}]_0$:$[\mathrm{Ti}_{\mathrm{complex}}]_0$ ratio of 200:1. Then toluene (40 mL) was added and the slurry was heated at 60 °C with regular swirling for 1 h or until the supernatant solution had discoloured. The coloured solid was allowed to settle, then the supernatant was decanted (or filtered), and the product dried under vacuum (1×10^{-2} mbar) at room temperature for at least 4 h to ensure all the solvent was removed.

sMAO-$^{\mathrm{Me2}}$SB($^{t\mathrm{Bu,Me}}$ArO,I*)TiCl$_2$ (1$_{\mathrm{sMAO}}$): 90% isolated yield.

sMAO-$^{\mathrm{Me2}}$SB($^{t\mathrm{Bu2}}$ArO,I*)TiCl$_2$ (2$_{\mathrm{sMAO}}$): 96% isolated yield.

^{13}C CPMAS NMR (100.6 MHz, 10 kHz)**:** δ –8 (AlO**Me**), 18 (Ar**Me**) 30 (C**Me**$_3$), 50 (Ti**Me**) 128 (**Ar**) ppm.

^{27}Al Hahn echo NMR (104.2 MHz, 20 kHz)**:** δ 426, 244, 64, –95, –349, –484 ppm.

^{29}Si CPMAS NMR (79.4 MHz, 10 kHz)**:** δ –13 (**Si**Me$_2$) ppm.

IR (KBr): 1026, 1086, 1219, 1259 1384, 1442, 1500, 1534, 1599, and 2947 (b) cm^{-1}.

SSMAO-$^{\mathrm{Me2}}$SB($^{t\mathrm{Bu2}}$ArO,I*)TiCl$_2$ (2$_{\mathrm{SSMAO}}$): 77% isolated yield.

^{1}H zgbs NMR (399.9 MHz, 20 kHz)**:** δ 6.8, 3.4, 2.0, 1.5, 0.9, 0.5, –0.2, –0.4, –1.1 ppm.

^{13}C CPMAS NMR (100.6 MHz, 10 kHz)**:** δ –10 (AlO**Me**), 31 (C**Me**), 50 (Ti**Me**), 128 (**Ar**) ppm.

^{27}Al Hahn echo NMR (104.2 MHz, 20 kHz)**:** δ 392, 259, 200, 33, –60, –132, –318 ppm.

^{29}Si CPMAS NMR (79.4 MHz, 10 kHz)**:** δ –13 (**Si**Me$_2$), –107 (**Si**O$_2$) ppm.

LDHMAO-$^{\mathrm{Me2}}$SB($^{t\mathrm{Bu2}}$ArO,I*)TiCl$_2$ (2$_{\mathrm{LDHMAO}}$): 61% isolated yield.

^{1}H zgbs NMR (399.9 MHz, 20 kHz)**:** δ 7.0, 6.8, 3.3, 2.0, 1.0, 0.5, –0.3, –0.4, –0.7 ppm.

^{13}C CPMAS NMR (100.6 MHz, 10 kHz)**:** δ –9, 12, 22, 26, 32, 35, 50, 62, 128, 164 ppm.

^{27}Al Hahn echo NMR (104.2 MHz, 20 kHz)**:** δ 596, 354, 231, 216, 86, 56, 28, –34, –154, –412, –571, –763 (Al in MAO) ppm.

^{27}Al DPMAS NMR (104.2 MHz, 20 kHz)**:** δ 67, 7 (Mg$_3$**Al** LDH) ppm.

^{29}Si CPMAS NMR (79.4 MHz, 10 kHz)**:** δ –14 (**Si**Me$_2$), –25, –102 ppm.

sMAO-$^{\mathrm{Me2}}$SB($^{t\mathrm{Bu2}}$ArO,I*)TiBr$_2$ (3$_{\mathrm{sMAO}}$): 60% isolated yield.

sMAO-$^{\mathrm{Me2}}$SB($^{t\mathrm{Bu2}}$ArO,I*)TiI$_2$ (4$_{\mathrm{sMAO}}$): 66% isolated yield.

sMAO-$^{\mathrm{Me2}}$SB($^{(\mathrm{CMe2Ph})2}$ArO,I*)TiCl$_2$ (5$_{\mathrm{sMAO}}$): 76% isolated yield.

sMAO-^{Me2}SB(^{tBu,Me}ArO,Ind)TiCl$_2$ (6$_{sMAO}$): 77% isolated yield.

Slurry-phase ethylene polymerisation studies. A typical slurry-phase laboratory polymerisation run was performed as follows. 150 mg triisobutylaluminium (TIBA) was added into a vial and 10 mL of hexanes was added. This mixture was introduced into a 150 mL Rotaflo ampoule containing a stirrer bar and swirled around the glassware. 10 mg supported catalyst was added to the ampoule and washed in with a further 40 mL hexanes. The vessel was sealed and was pumped on to a vacuum line and degassed under reduced pressure. It was cycled a further three times using an ethylene purge while the reaction was brought to temperature in an oil bath with the stirring was set at 1000 rpm. The stopcock was opened to ethylene at a pressure of 2 bar and the timer was started. On completion of the run, the vessel was closed to ethylene and degassed, then filtered on a glass sintered frit (porosity 3) and washed with 2 × 25 mL pentane. The polyethylene (PE) was dried under vacuum until constant weight. All polymerisation runs were carried out at least in duplicate to ensure reproducibility.

Solution-phase ethylene polymerisation studies. A stock solution of complex in toluene was prepared at a concentration of 713 µM. 1000 equivalents MAO were added to a 150 ml Rotaflo ampoule and washed in with 9 mL hexanes. 1 ml stock solution (414 µg, 713 nmol) was added to the ampoule along with a further 40 mL hexanes. The run was continued as above.

3. Single-crystal X-ray crystallography

3.1 Tables

Table S 1 Selected bond lengths (Å) and angles (°).

	(**2**)
Ti(1)–O(1)	1.7838(1)
Ti(1)–I^*_{CENT}	2.0156(1)
Ti(1)–C(1)	2.2697(1)
Ti(1)–Cl(1)	2.2632(1)
Ti(1)–Cl(2)	2.2734(1)
Si(1)–C(1)	1.9058(1)
Si(1)–C(23)	1.8987(1)
C(1)–Si(1)–C(23)	107.07(1)
I^*_{CENT}–Ti(1)–O(1)	
C(1)–Si(1)–C(23)–C(18)	35.89(1)
Ti(1)–O(1)–C(18)–C(23)	27.86(1)
I*–ArO[a]	48.57

[a] angle formed between Cp(I*) and Ph(ArO) planes

Table S 2 Selected experimental crystallographic data.

Chemical formula	$C_{31}H_{44}Cl_2OSiTi$
M_r	579.55
Chemical system, space group	Triclinic, $P\overline{1}$
Temperature (K)	150
a, *b*, *c* (Å)	8.7639(2), 14.1232(2), 14.1951(4)
α, *β*, *γ* (°)	116.403(2), 90.929(2), 104.547(2)
V (Å^3)	1506.59(7)
Z	2
Radiation type	Cu *K*α
μ (mm^{-1})	4.58
Crystal size (mm)	0.21, 0.18, 0.07
Diffractometer	SuperNova, Dual, Cu at home/near, Atlas
Absorption correction	Multi-scan *CrysAlisPro* 1.171.39.46 (Rigaku Oxford Diffraction, 2018). Empirical absorption correction using spherical harmonics, implemented in SCALE3 ABSPACK scaling algorithm.
T_{min}, T_{max}	0.804, 1.000
Number of measured, independent, and observed [$I > 2\sigma(I)$] reflections	27747, 6147, 5606
R_{int}	0.037
$(\sin \theta/\lambda)_{max}$ (Å^{-1})	0.625
$R[F^2 > 2\sigma(F^2)]$, $wR(F^2)$, S	0.043, 0.122, 1.04
No. of reflections	6147
No. of parameters	339
No. of restraints	0
H-atom treatment	H-atom parameters constrained
$(\Delta/\sigma)_{max}$	0.001
$\Delta\rangle_{max}$, $\Delta\rangle_{min}$ (e Å^{-3})	0.58, –0.31
CCDC Deposition Number	2090028

3.2 Molecular structure illustrations

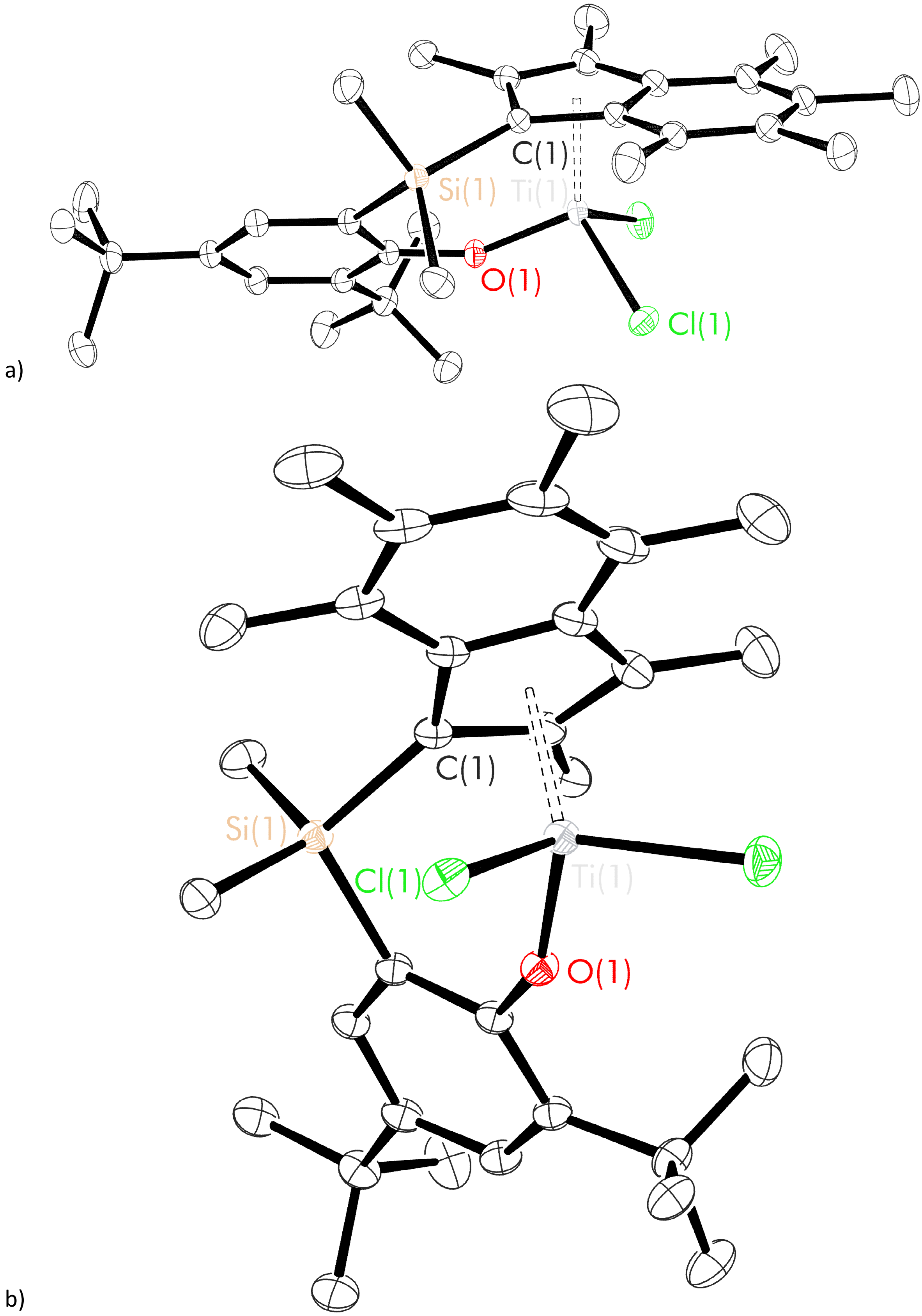

Fig. S 1 Thermal displacement ellipsoid drawings (30% probability) of ^{Me2}SB($^{\mathit{t}Bu2}$ArO,I*)TiCl$_2$ (**2**). All hydrogen atoms omitted for clarity.

4. NMR spectroscopy

4.1 Solution NMR spectroscopy of complexes

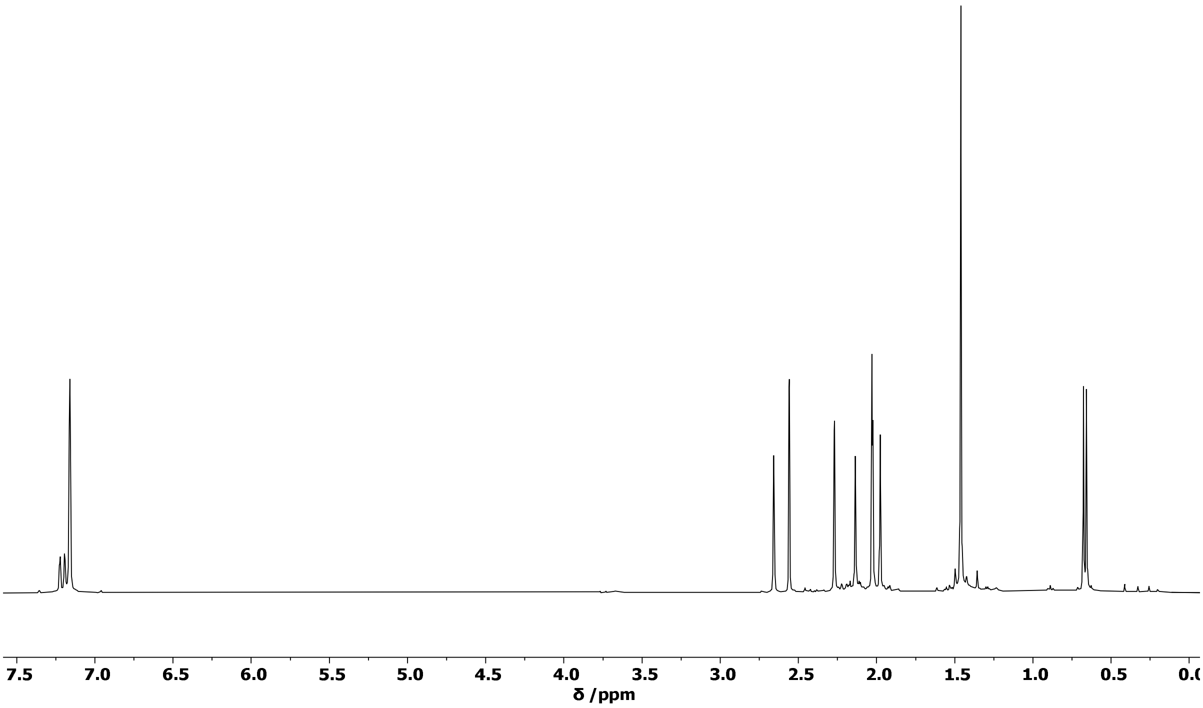

Fig. S 2 ^{1}H NMR spectrum of ^{Me2}SB(^{tBu,Me}ArO,I*)TiCl$_2$ (**1**) (benzene-d_6, 400 MHz, 298 K).

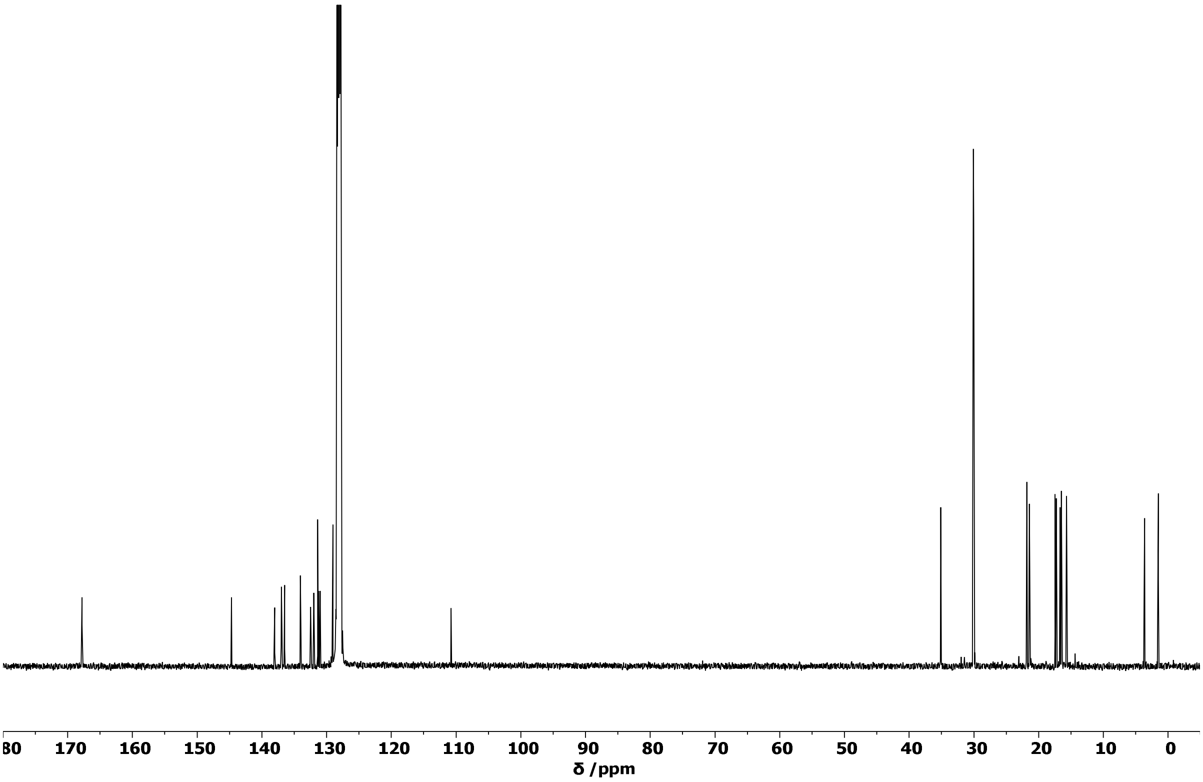

Fig. S 3 ^{13}C{^{1}H} NMR spectrum of ^{Me2}SB(^{tBu,Me}ArO,I*)TiCl$_2$ (**1**) (benzene-d_6, 126 MHz, 298 K).

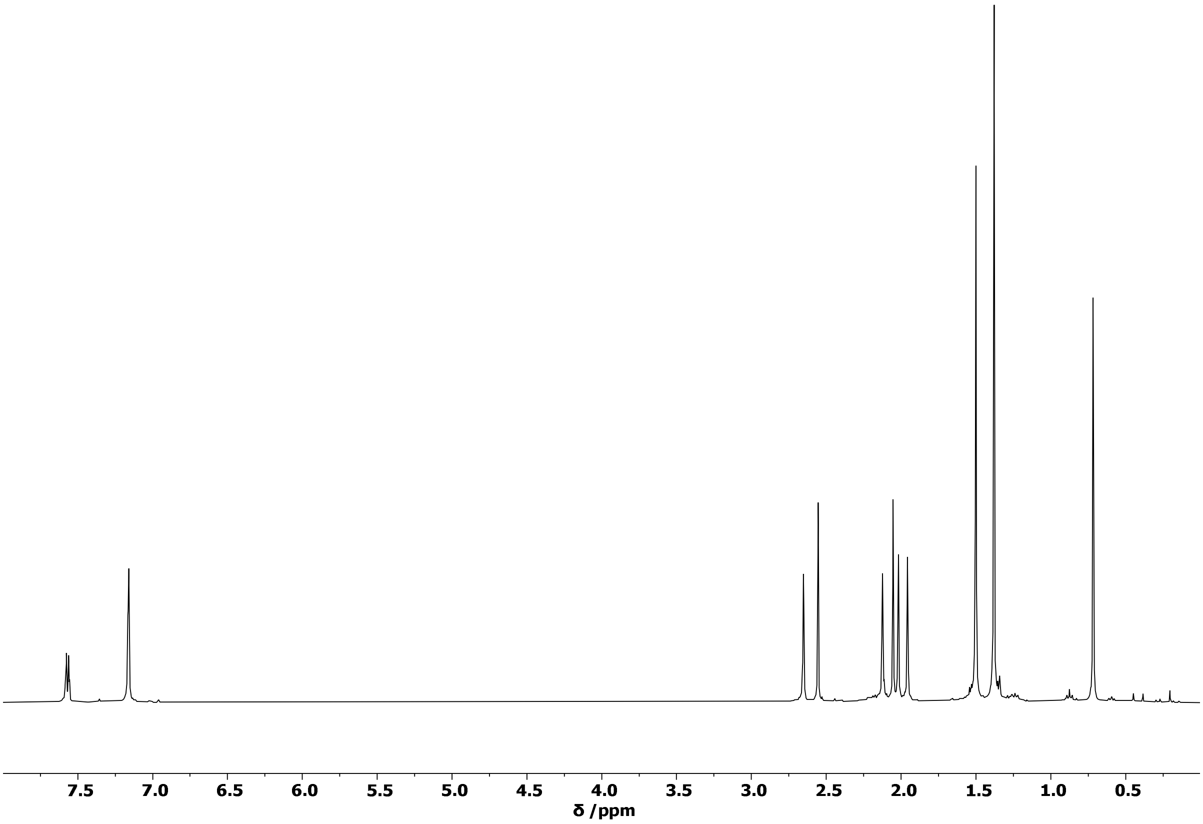

Fig. S 4 ^{1}H NMR spectrum of ^{Me2}SB($^{^t Bu2}$ArO,I*)TiCl$_2$ (**2**) (benzene-*d*$_6$, 400 MHz, 298 K).

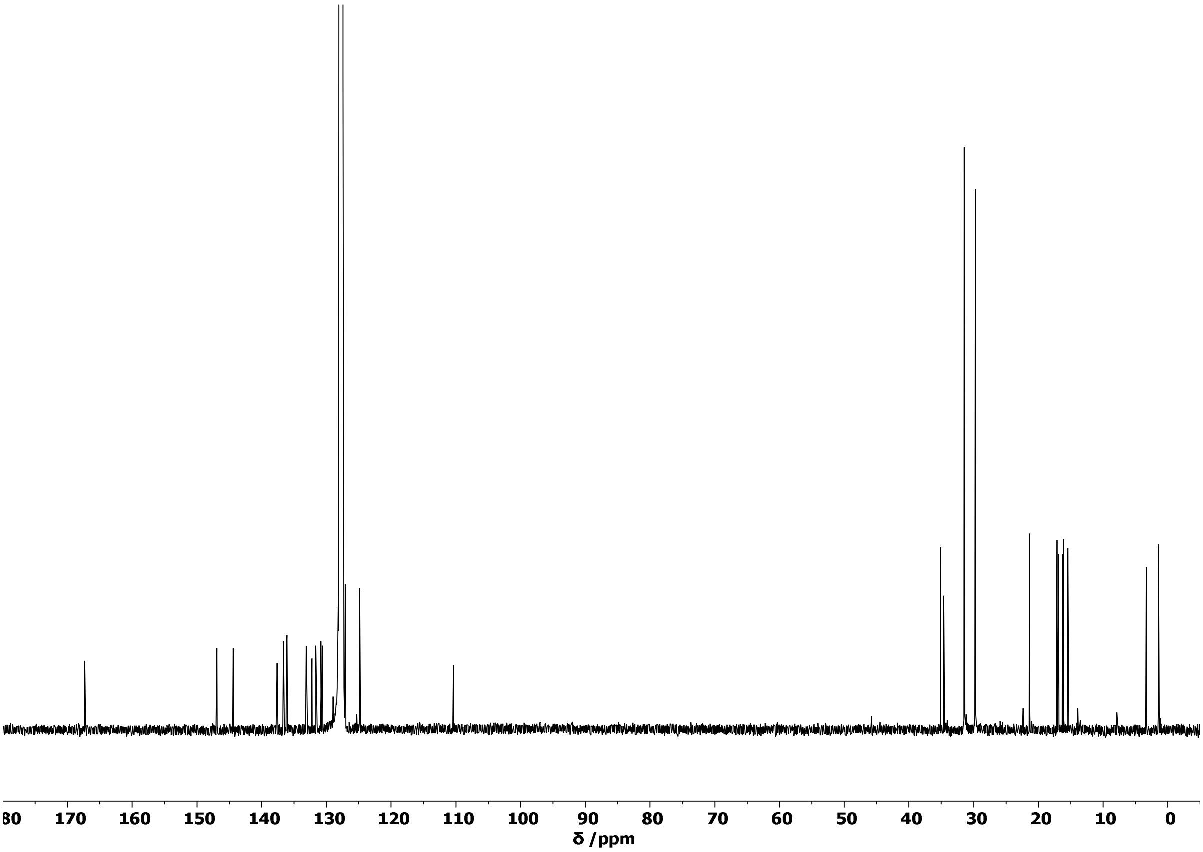

Fig. S 5 ^{13}C{^{1}H} NMR spectrum of ^{Me2}SB($^{^t Bu2}$ArO,I*)TiCl$_2$ (**2**) (benzene-*d*$_6$, 126 MHz, 298 K).

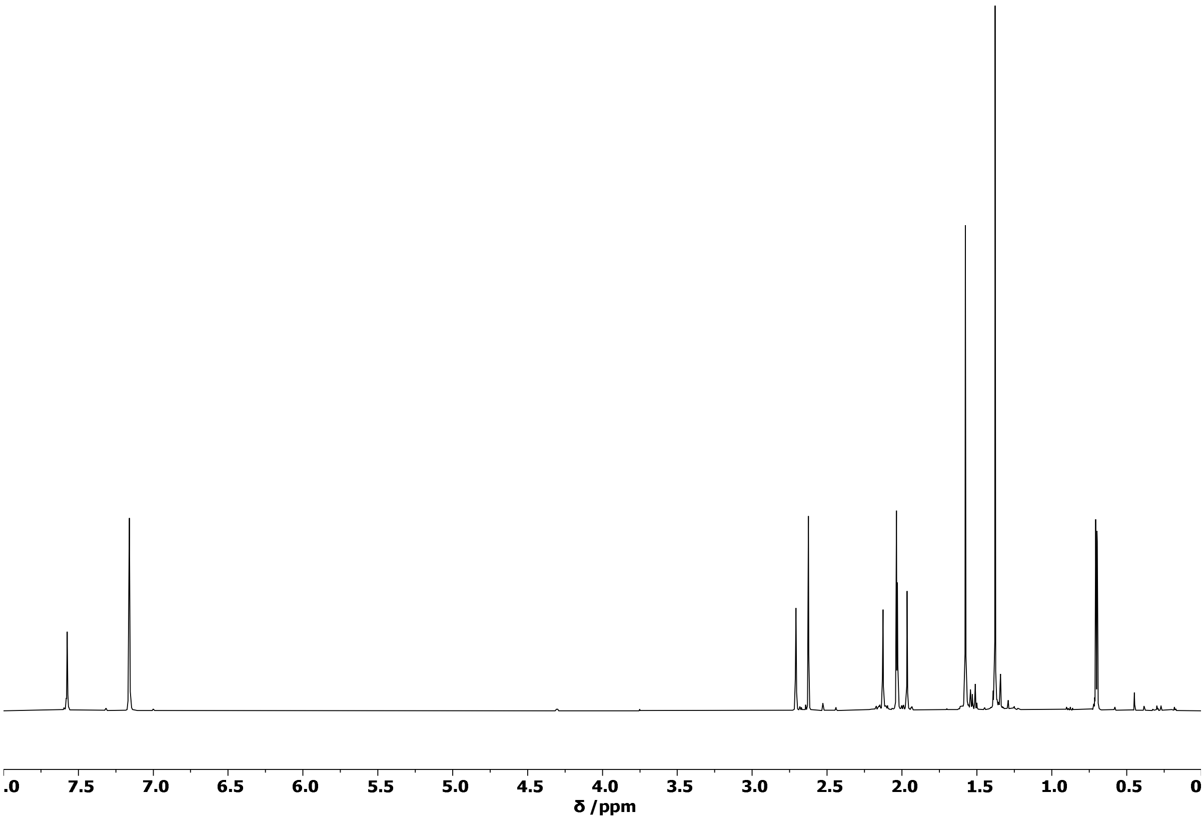

Fig. S 6 ^{1}H NMR spectrum of $^{\mathrm{Me2}}$SB($^{t\mathrm{Bu2}}$ArO,I*)TiBr$_2$ (**3**) (benzene-d_6, 500 MHz, 298 K).

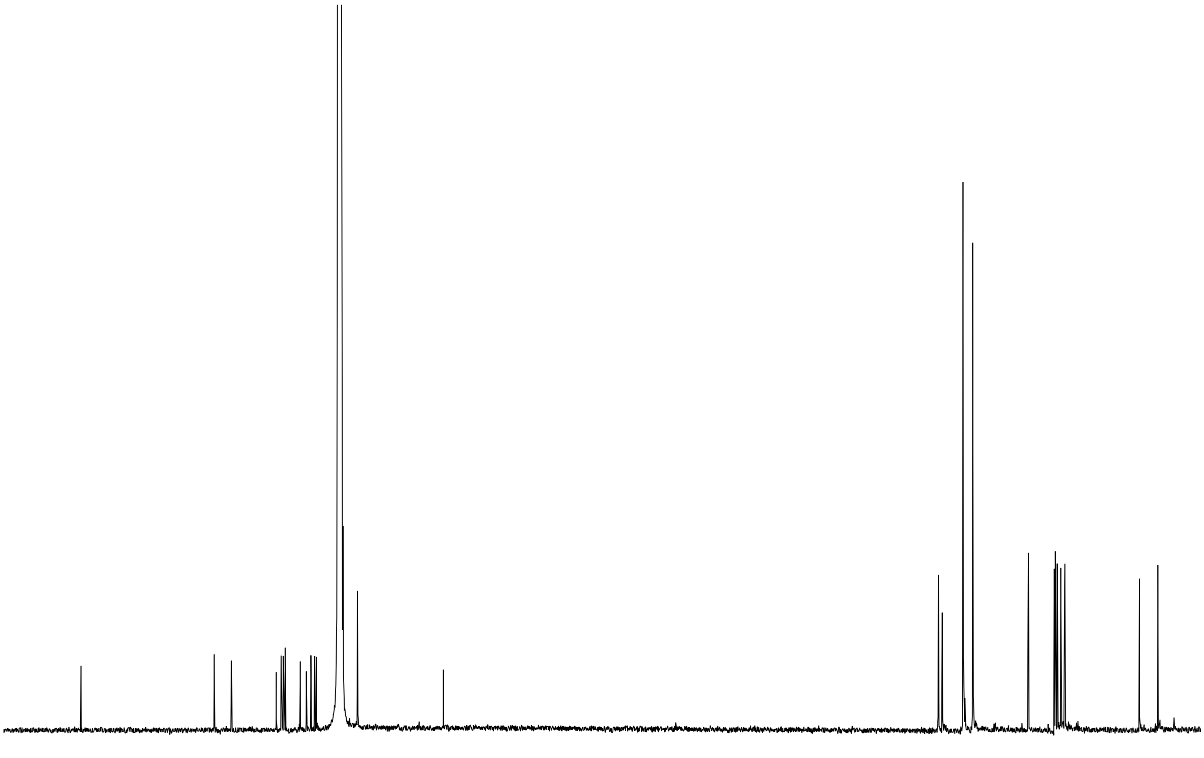

Fig. S 7 ^{13}C{^{1}H} NMR spectrum of $^{\mathrm{Me2}}$SB($^{t\mathrm{Bu2}}$ArO,I*)TiBr$_2$ (**3**) (benzene-d_6, 126 MHz, 298 K).

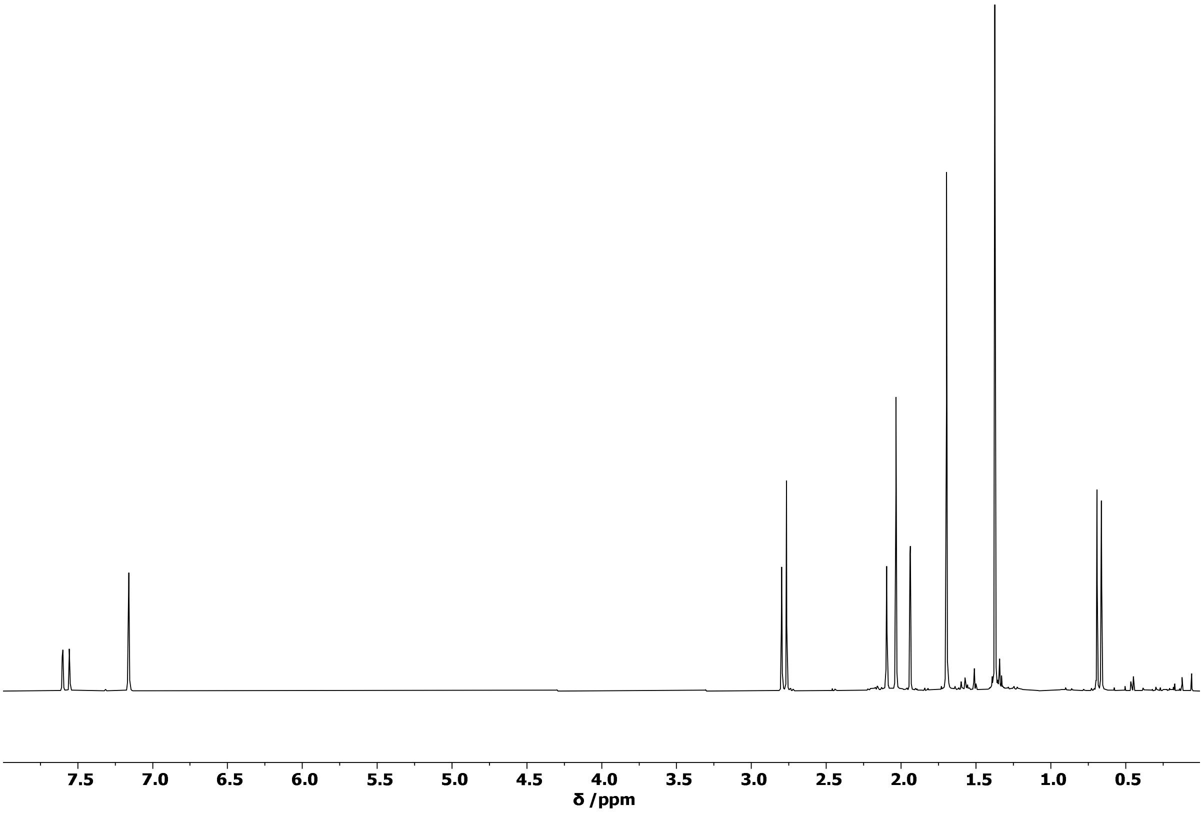

Fig. S 8 ^{1}H NMR spectrum of ^{Me2}SB($^{^t\!Bu2}$ArO,I*)TiI$_2$ (**4**) (benzene-*d*$_6$, 500 MHz, 298 K).

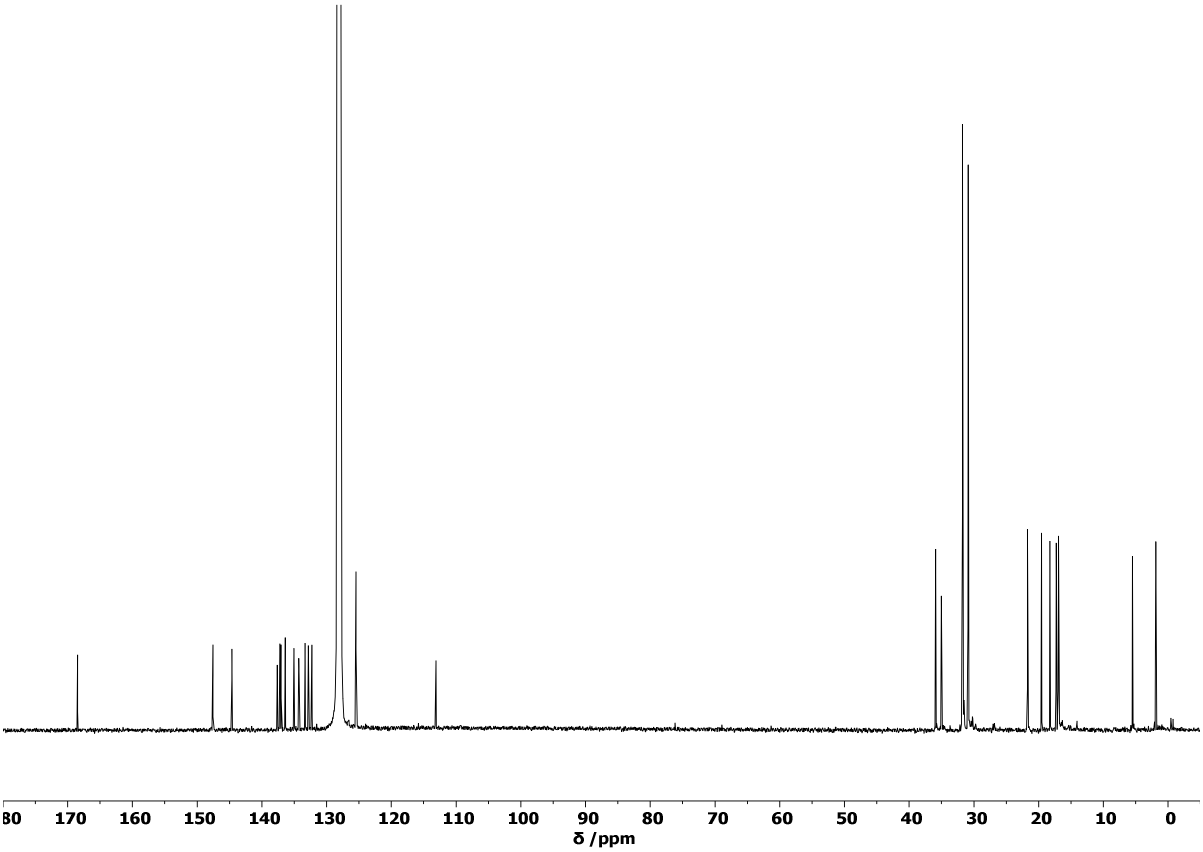

Fig. S 9 ^{13}C{^{1}H} NMR spectrum of ^{Me2}SB($^{^t\!Bu2}$ArO,I*)TiI$_2$ (**4**) (benzene-*d*$_6$, 126 MHz, 298 K).

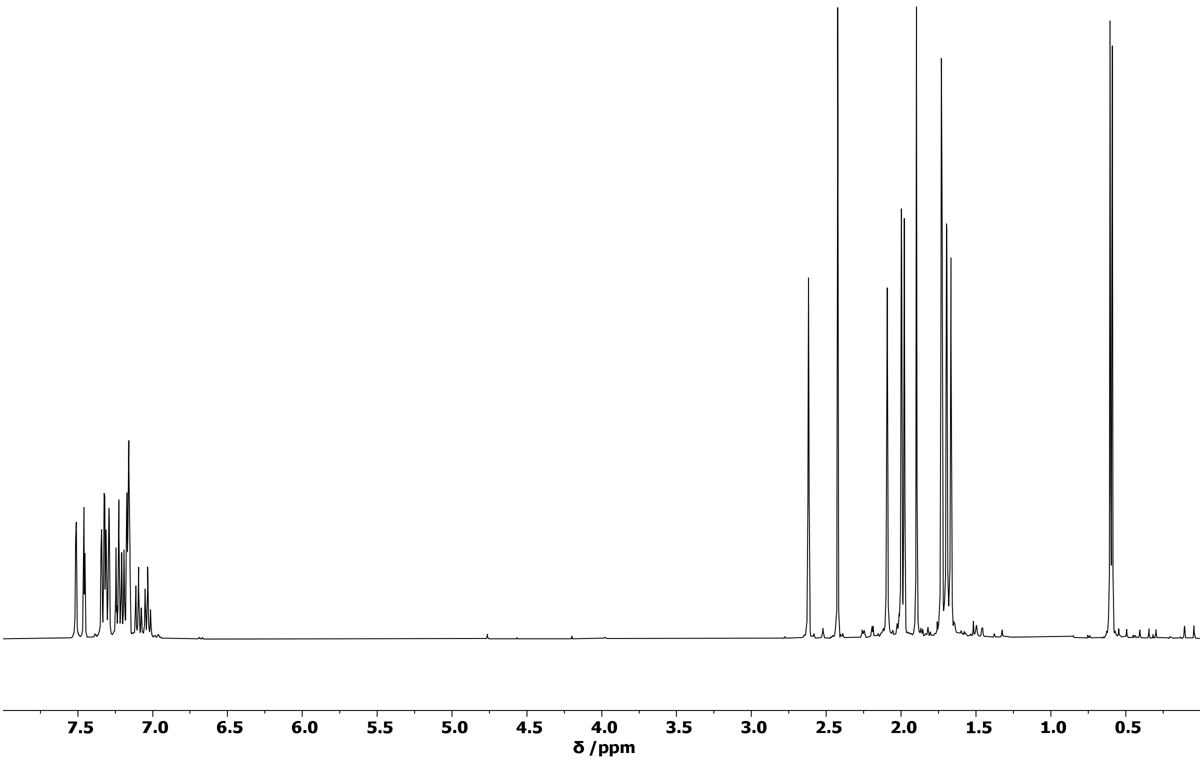

Fig. S 10 ^{1}H NMR spectrum of ^{Me2}SB($^{(CMe2Ph)2}$ArO,I*)TiCl$_2$ (**5**) (benzene-d_6, 400 MHz, 298 K).

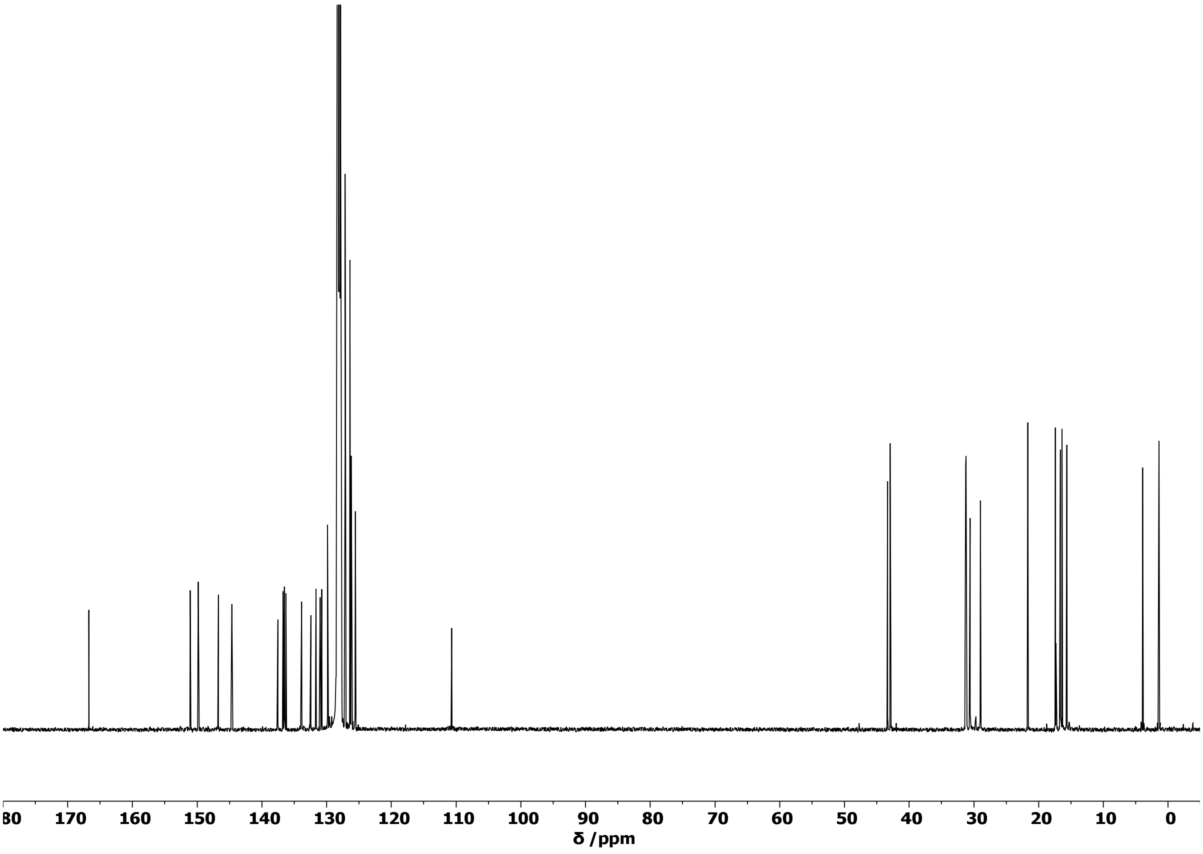

Fig. S 11 ^{13}C{^{1}H} NMR spectrum of ^{Me2}SB($^{(CMe2Ph)2}$ArO,I*)TiCl$_2$ (**5**) (benzene-d_6, 126 MHz, 298 K).

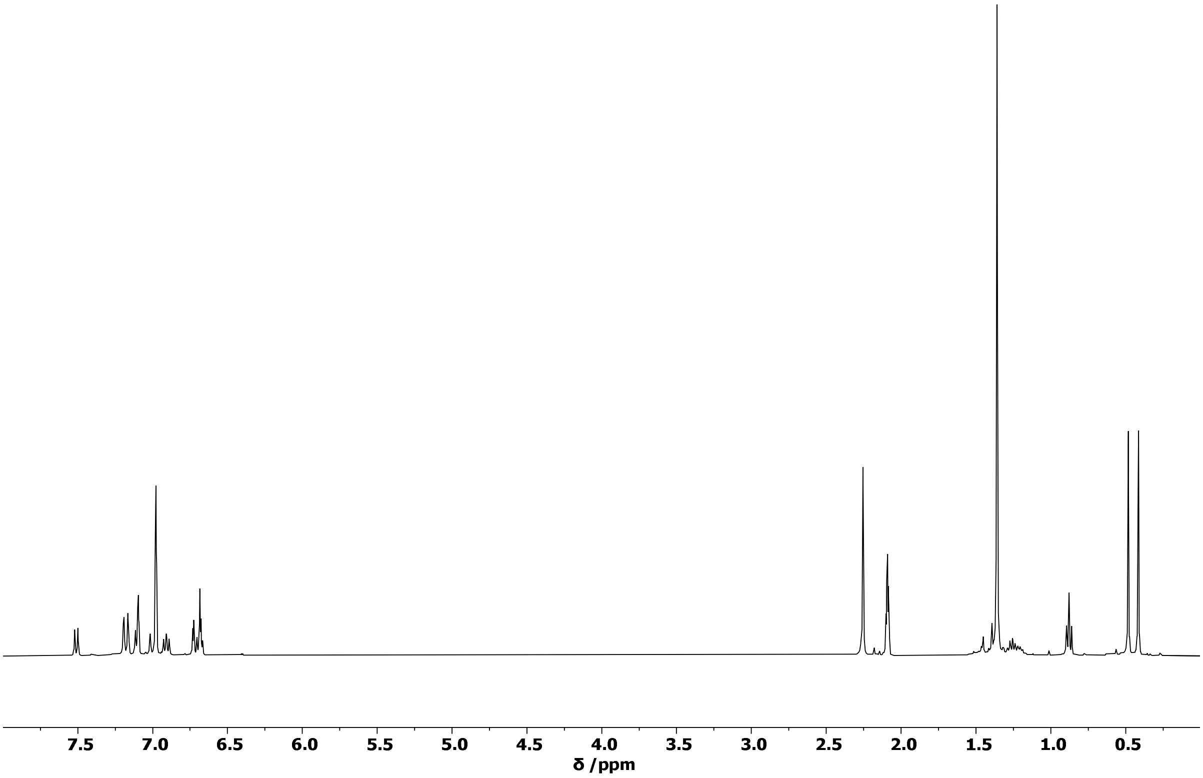

Fig. S 12 ^{1}H NMR spectrum of ^{Me2}SB($^{t\mathrm{Bu,Me}}$ArO,Ind)TiCl$_2$ (**6**) (toluene-d_8, 400 MHz, 298 K).

4.2 Solid-state NMR spectroscopy of solid catalysts

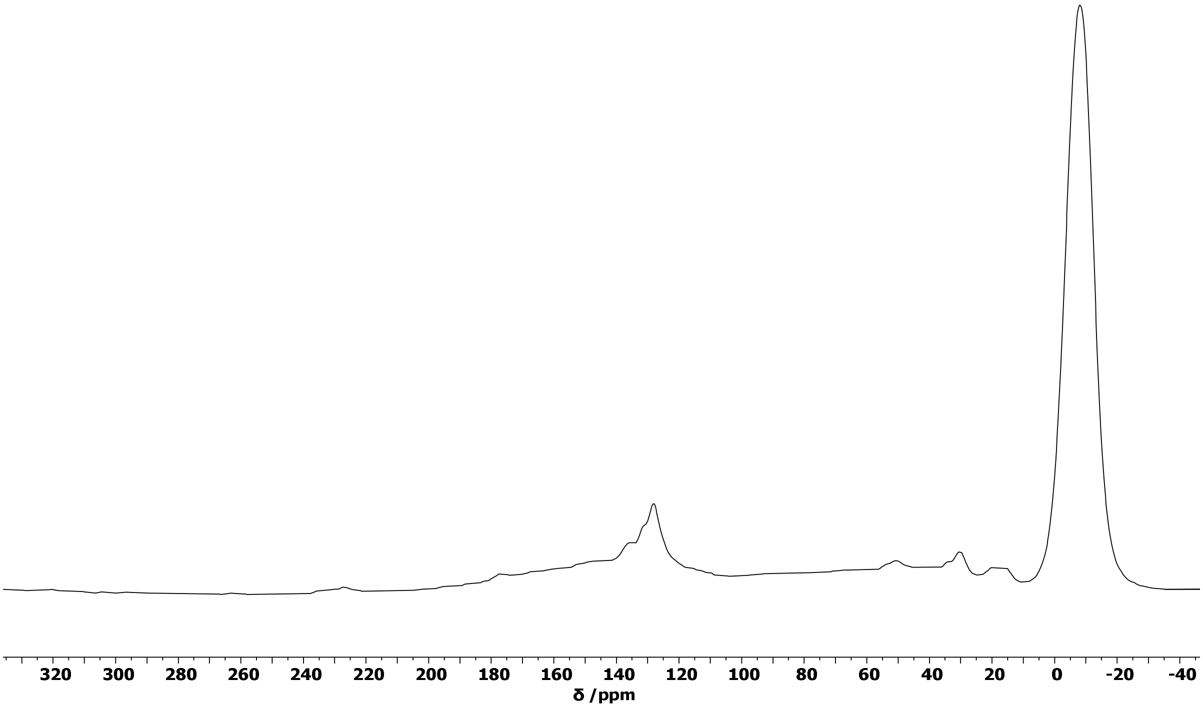

Fig. S 13 ^{13}C CPMAS ssNMR spectrum of sMAO-^{Me2}SB($^{t\mathrm{Bu2}}$ArO,I*)TiCl$_2$ (**2$_{sMAO}$**) (10 kHz, 101 MHz, 298 K).

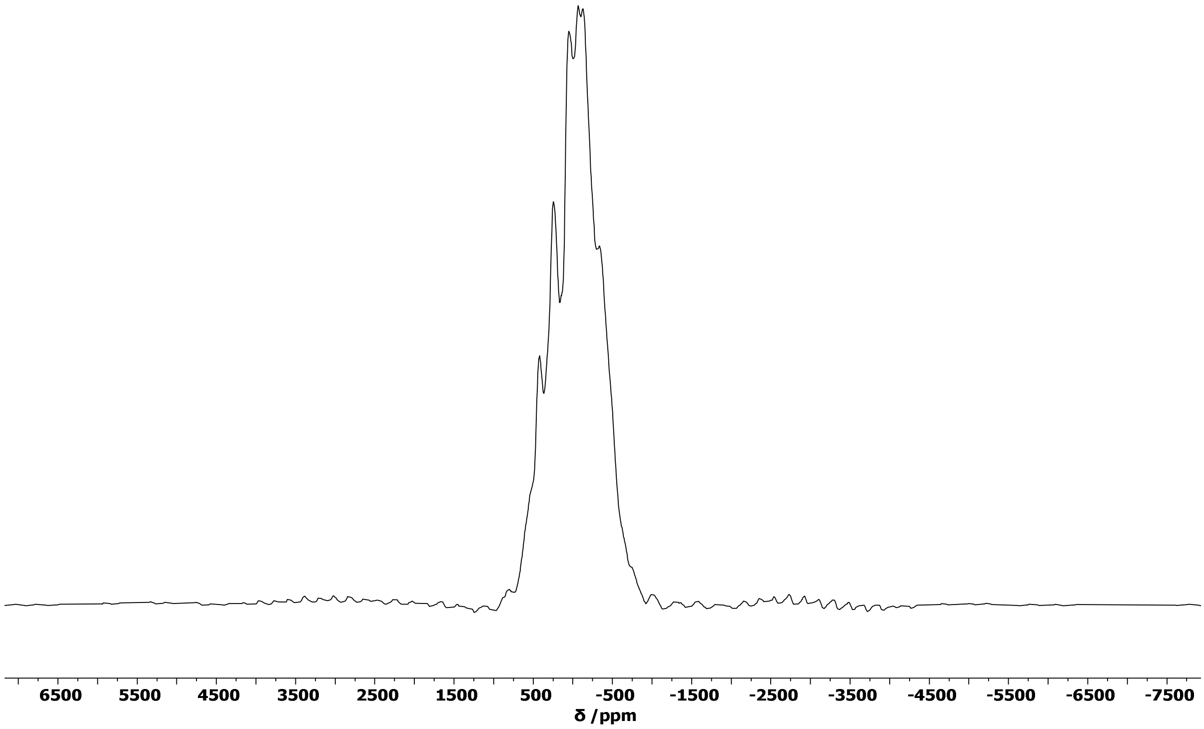

Fig. S 14 ^{27}Al Hahn echo ssNMR spectrum of sMAO-$^{\mathrm{Me2}}$SB($^{t\mathrm{Bu2}}$ArO,I*)TiCl$_2$ (**2**$_{\mathbf{sMAO}}$) (20 kHz, 104 MHz, 298 K).

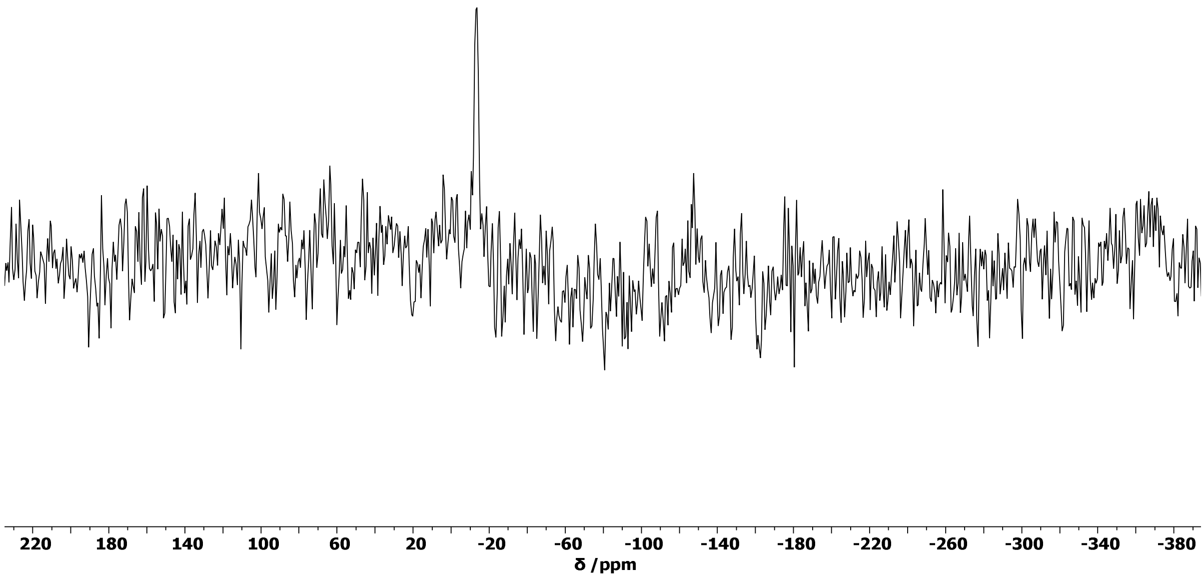

Fig. S 15 ^{29}Si CPMAS ssNMR spectrum of sMAO-$^{\mathrm{Me2}}$SB($^{t\mathrm{Bu2}}$ArO,I*)TiCl$_2$ (**2**$_{\mathbf{sMAO}}$) (10 kHz, 79 MHz, 298 K).

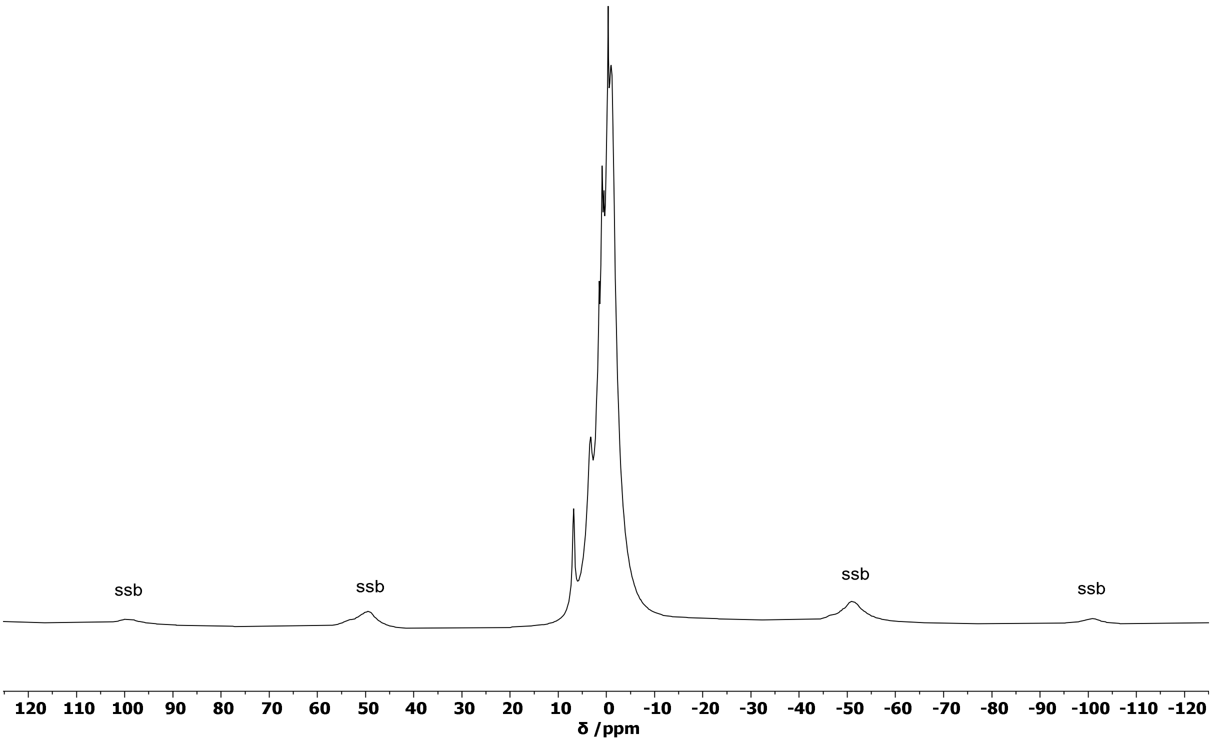

Fig. S 16 ^{1}H ssNMR spectrum of SSMAO-^{Me2}SB(^{tBu2}ArO,I*)TiCl$_2$ (**2_{SSMAO}**) (20 kHz, 399.9 MHz, 298 K). Spinning side bands denoted ssb.

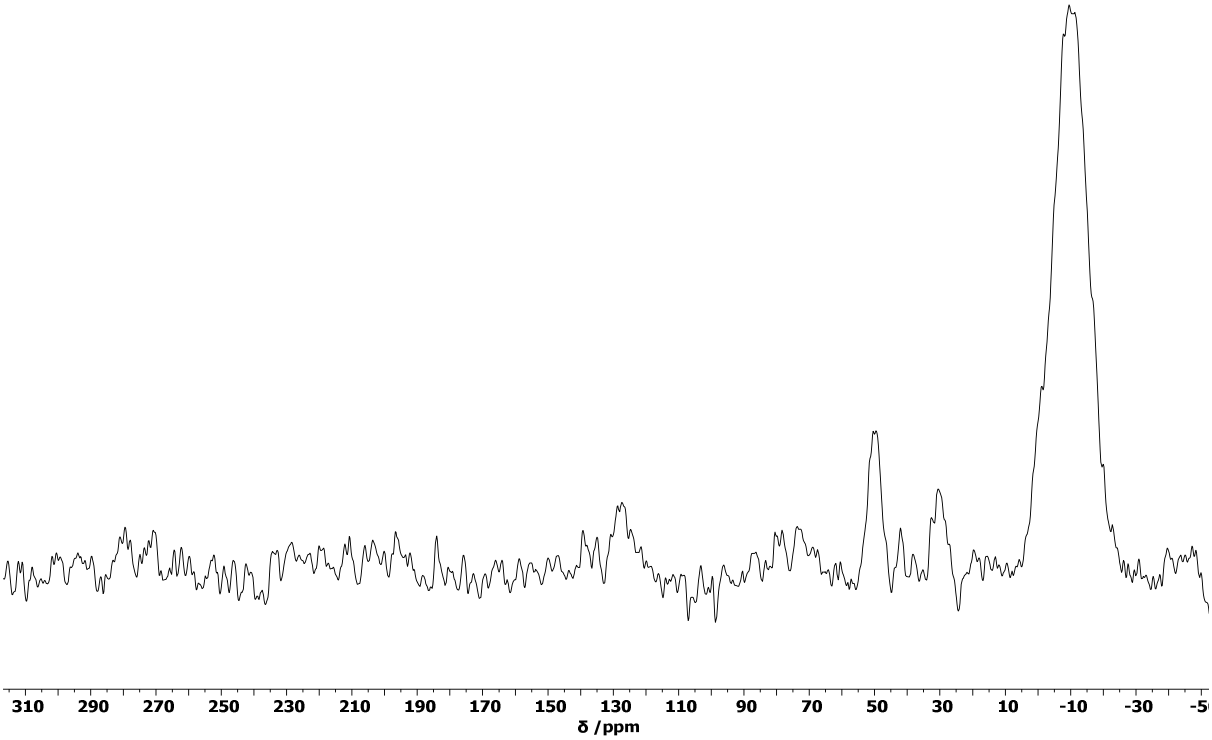

Fig. S 17 ^{13}C CPMAS ssNMR spectrum of SSMAO-^{Me2}SB(^{tBu2}ArO,I*)TiCl$_2$ (**2_{SSMAO}**) (10 kHz, 101 MHz, 298 K).

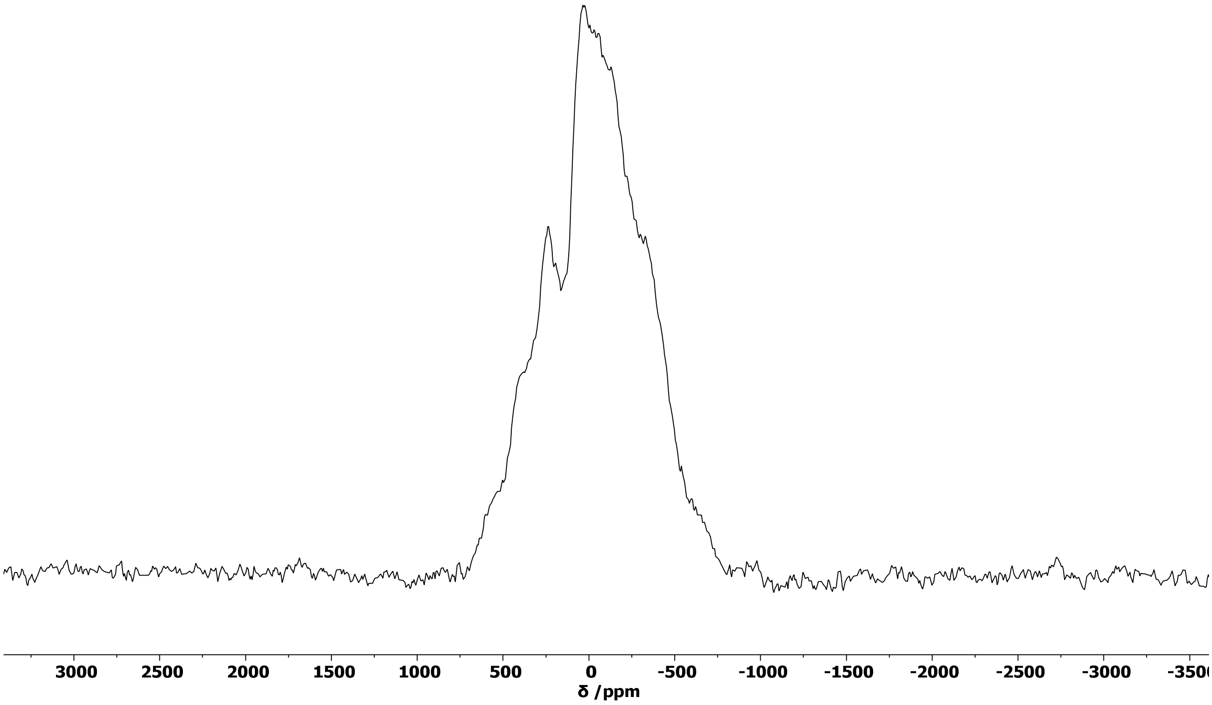

Fig. S 18 ^{27}Al Hahn echo ssNMR spectrum of SSMAO-^{Me2}SB($^{t\mathrm{Bu}2}$ArO,I*)TiCl$_2$ (**2$_{\mathbf{SSMAO}}$**) (20 kHz, 104 MHz, 298 K).

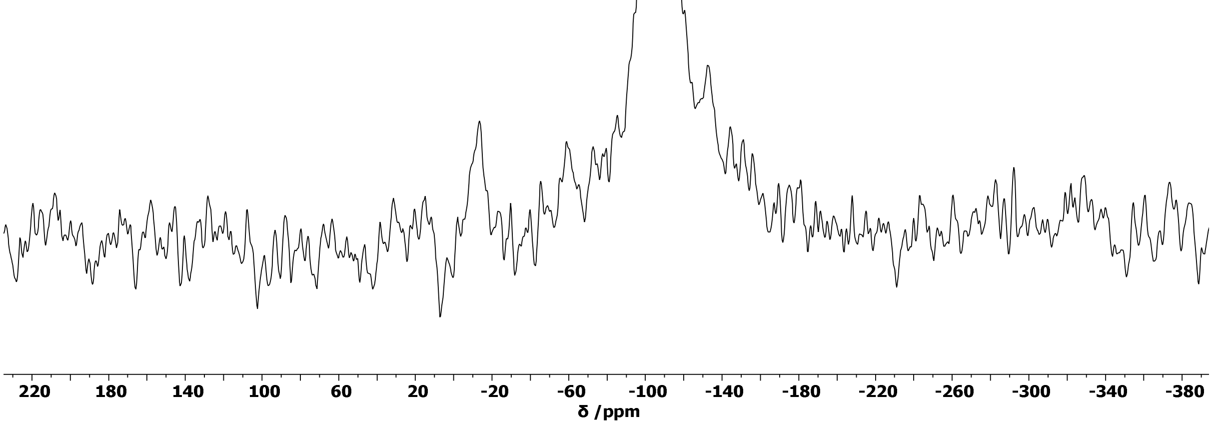

Fig. S 19 ^{29}Si CPMAS ssNMR spectrum of SSMAO-^{Me2}SB($^{t\mathrm{Bu}2}$ArO,I*)TiCl$_2$ (**2$_{\mathbf{SSMAO}}$**) (10 kHz, 79 MHz, 298 K).

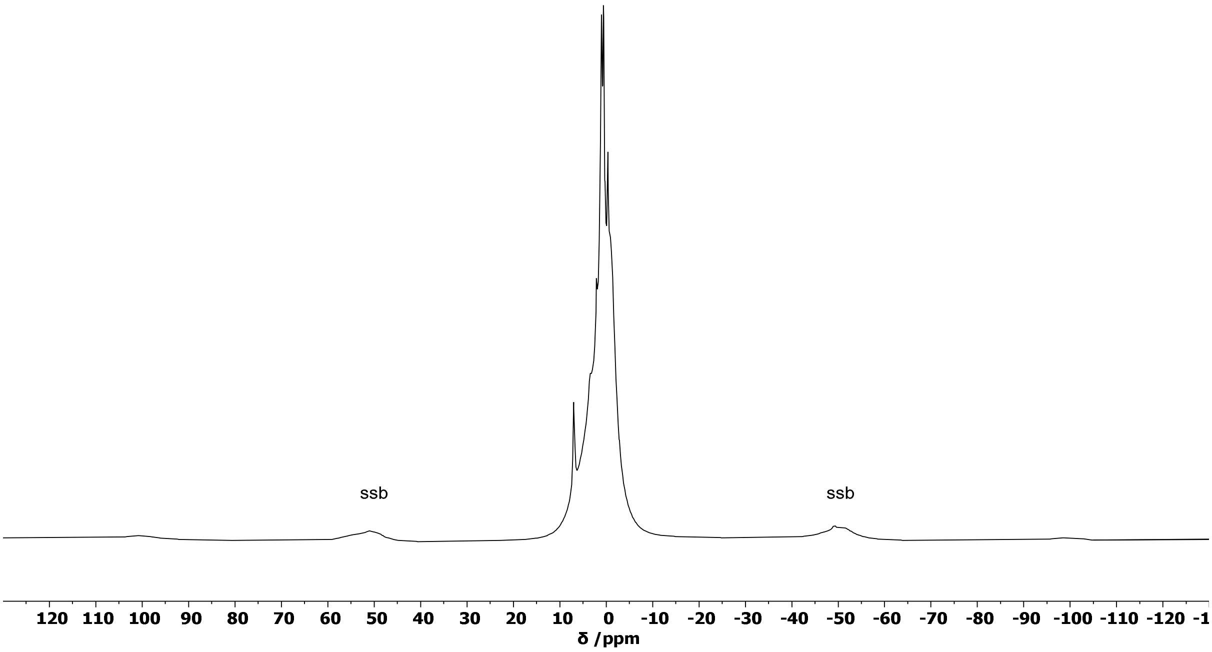

Fig. S 20 ^{1}H ssNMR spectrum of LDHMAO-^{Me2}SB(^{tBu2}ArO,I*)TiCl$_2$ (**2**$_{\mathbf{LDHMAO}}$) (20 kHz, 399.9 MHz, 298 K). Spinning side bands denoted ssb.

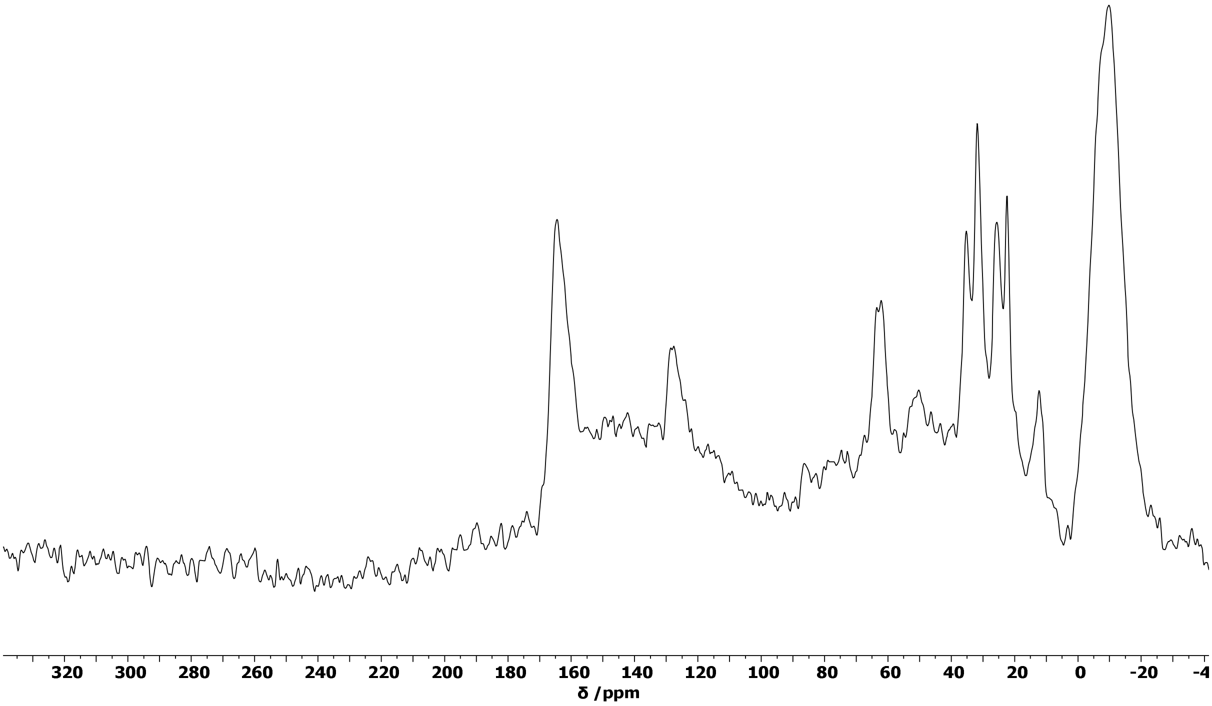

Fig. S 21 ^{13}C CPMAS ssNMR spectrum of LDHMAO-^{Me2}SB(^{tBu2}ArO,I*)TiCl$_2$ (**2**$_{\mathbf{LDHMAO}}$) (10 kHz, 101 MHz, 298 K).

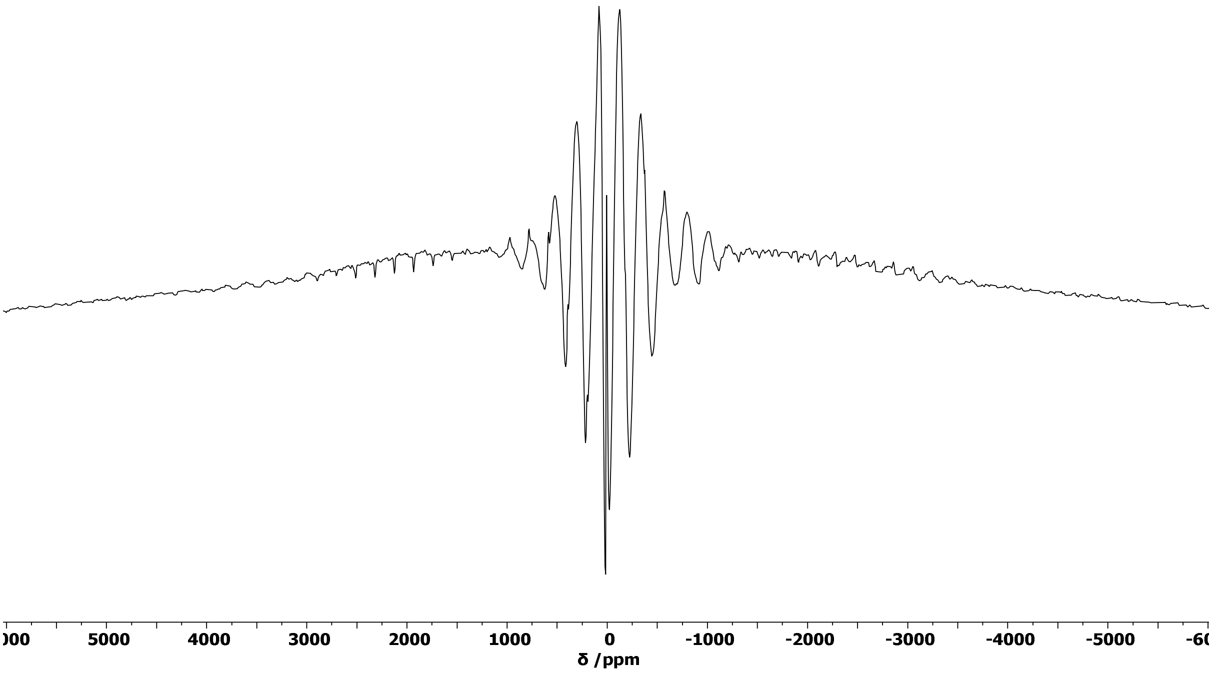

Fig. S 22 ^{27}Al Hahn echo ssNMR spectrum of LDHMAO-^{Me2}SB(^{tBu2}ArO,I*)TiCl$_2$ (**2$_{LDHMAO}$**) (20 kHz, 104 MHz, 298 K).

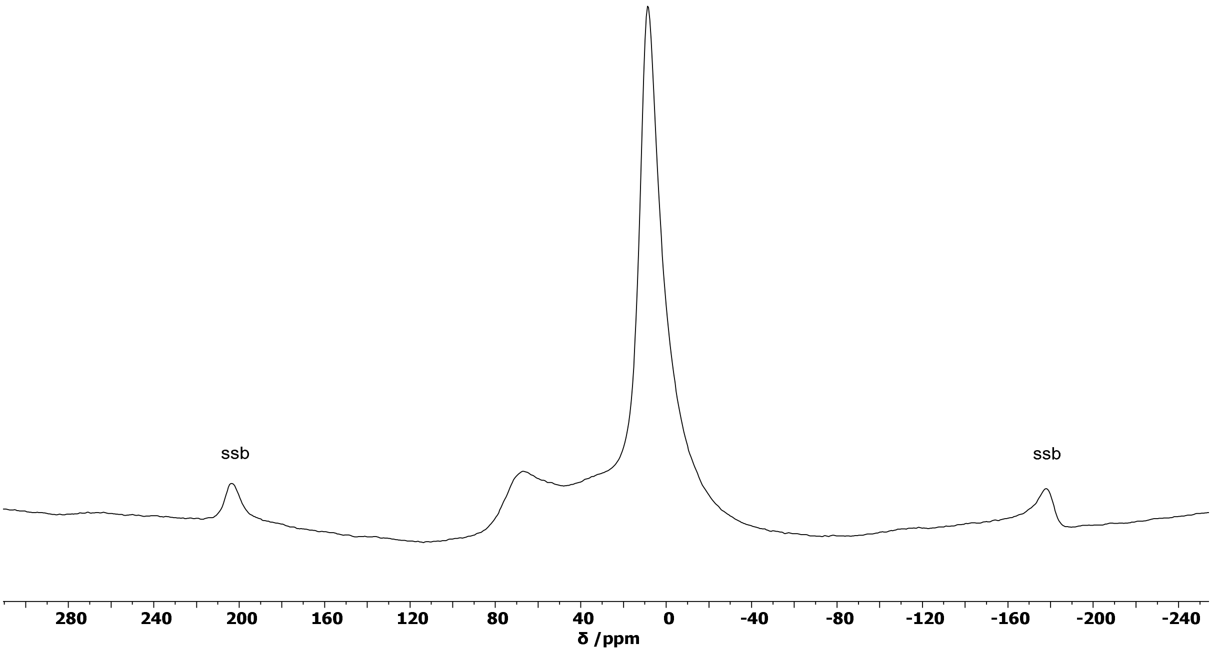

Fig. S 23 ^{27}Al DPMAS ssNMR spectrum of LDHMAO-^{Me2}SB(^{tBu2}ArO,I*)TiCl$_2$ (**2$_{LDHMAO}$**) (20 kHz, 104 MHz, 298 K). Spinning side bands denoted ssb.

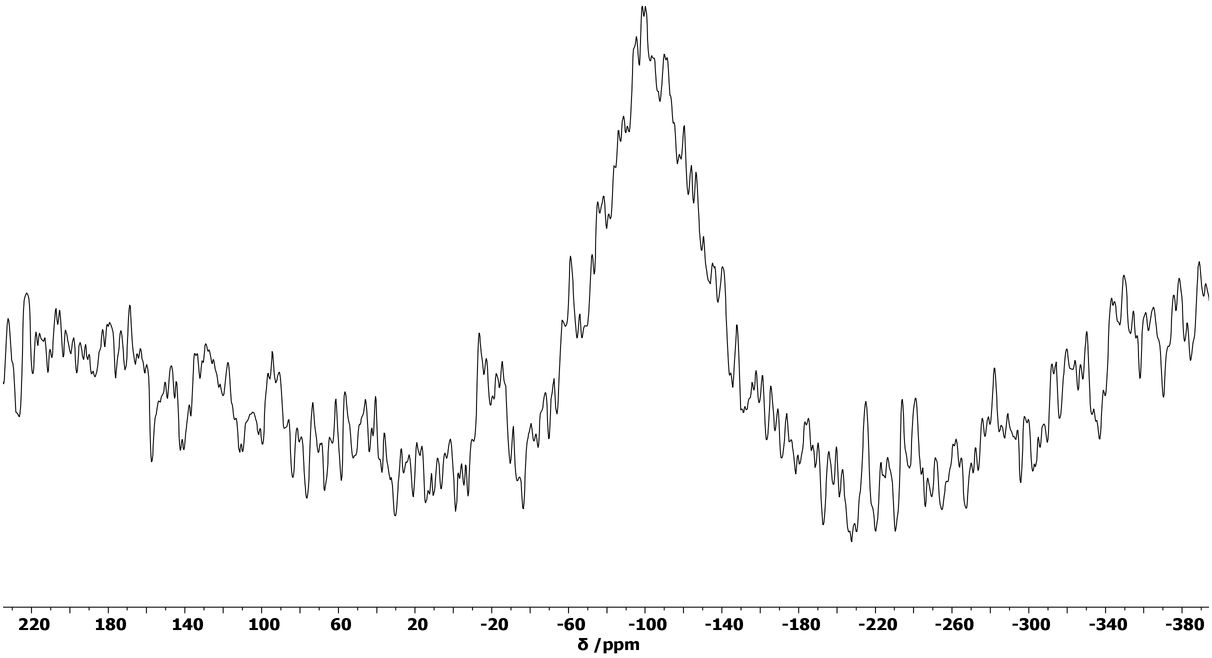

Fig. S 24 ^{29}Si CPMAS ssNMR spectrum of LDHMAO-^{Me2}SB(^{tBu2}ArO,I*)TiCl$_2$ (**2**$_{\mathbf{LDHMAO}}$) (10 kHz, 79 MHz, 298 K).

5. Polymerisation studies

5.1 Solution-phase polymerisation

Complex	Temperature /°C	Time /mins	Activity /kg mol$_{Ti}^{-1}$ h^{-1} bar^{-1}
2	30	5	1079 ± 53
	40	5	1474 ± 53
	50	5	2586 ± 914
	60	5	3842 ± 825
	70	5	4774 ± 707
	80	5	4501 ± 1247
	90	5	3602 ± 618

Table S 3 Polymerisation conditions: [Al$_{MAO}$]$_0$/[Ti]$_0$ = 1000, 2 bar ethylene, 414 µg catalyst, 49 mL hexanes, 1 mL toluene, 60 °C, and 5 minutes.

5.2 Slurry-phase polymerisation

Catalyst	Temperature /°C	Time /mins	Activity /kg mol$_{Ti}^{-1}$ h^{-1} bar^{-1}	M_w /kDa	PDI
2$_{\mathbf{sMAO}}$	30	30	2834 ± 338	3376.0	3.4
	40	30	3518 ± 129	3117.2	4.4
	50	30	3614 ± 123	2352.6	4.4
	60	30	3719 ± 106	2087.5	5.2
	70	30	3367 ± 151	2033.7	5.5
	80	30	2450 ± 121	1550.9	6.9

	90	30	2180 ± 17	1516.9	6.4
2$_{\mathrm{SSMAO}}$	30	30	236 ± 24	2567.9	2.0
	40	30	327 ± 8	2821.1	2.0
	50	30	311 ± 89	2692.2	2.0
	60	30	437 ± 21	2643.8	1.7
	70	30	446 ± 44	2619.5	2.2
	80	30	430 ± 15	2287.5	2.8
	90	30	310 ± 1	2023.9	3.8
2$_{\mathrm{LDHMAO}}$	30	30	642 ± 49	4195.0	1.7
	40	30	732 ± 27	4081.6	1.8
	50	30	871 ± 91	4200.9	1.6
	60	30	872 ± 95	-	-
	70	30	820 ± 73	3893.7	1.8
	80	30	638 ± 84	3370.0	2.8
	90	30	619 ± 29	3230.0	2.7

Table S 4 Polymerisation conditions: $[\mathrm{Al}_{\mathrm{support}}]_0/[\mathrm{Ti}]_0$ = 200, 150 mg TIBA, 2 bar ethylene, 10 mg catalyst, 50 mL hexanes, 60 °C, and 30 minutes.

Catalyst	**Temperature /°C**	**Time /mins**	**Activity /kg $\mathrm{mol_{Ti}^{-1}\ h^{-1}\ bar^{-1}}$**	**M_w /kDa**	**PDI**
1$_{\mathrm{sMAO}}$	50	30	3078 ± 34	2513.8	2.8
	60	30	3231 ± 150	2087.9	3.0
	70	30	2776 ± 190	1876.4	3.8
	80	30	2674 ± 70	1494.5	5.1
	90	30	1723 ± 192	1313.6	5.7
3$_{\mathrm{sMAO}}$	50	30	3126 ± 86	2631.2	2.3
	60	30	3133 ± 33	2437.7	3.0
	70	30	2984 ± 16	2184.5	3.1
	80	30	2881 ± 365	1491.5	4.2
	90	30	2186 ± 50	1385.0	5.0
4$_{\mathrm{sMAO}}$	50	30	2345 ± 42	2768.4	2.1
	60	30	2493 ± 263	2696.2	2.6
	70	30	2548 ± 130	2303.2	3.4
	80	30	2103 ± 186	1970.1	4.0
	90	30	1583 ± 68	1443.8	5.1
5$_{\mathrm{sMAO}}$	50	30	2114 ± 2	1862.5	3.5
	60	30	1983 ± 39	1777.0	3.5
	70	30	1597 ± 126	1392.8	3.7
	80	30	1317 ± 297	1108.2	3.9
	90	30	1022 ± 154	873.5	3.7
6$_{\mathrm{sMAO}}$	50	30	155 ± 3	1192.2	25.5
	60	30	144 ± 2	1091.7	20.9
	70	30	114 ± 16	878.2	23.7
	80	30	103 ± 13	719.5	35.9
	90	30	60 ± 7	501.5	20.8

Table S 5 Polymerisation conditions: $[\mathrm{Al_{sMAO}}]_0/[\mathrm{Ti}]_0 = 200$, 150 mg TIBA, 2 bar ethylene, 10 mg catalyst, 50 mL hexanes, 60 °C, and 30 minutes.

Catalyst	**Temperature /°C**	**Time /mins**	**Activity /kg $\mathrm{mol_{Ti}^{-1}\ h^{-1}\ bar^{-1}}$**	**M_w /kDa**	**PDI**
2$_{\mathrm{sMAO}}$ **/ TIBA**	60	30	3719 ± 106	2087.5	5.2
2$_{\mathrm{sMAO}}$ **/ TEA**	60	30	721 ± 312	791.1	14.1
2$_{\mathrm{sMAO}}$ **/ TMA**	60	30	1099 ± 8	1355.2	7.9
2$_{\mathrm{sMAO}}$ **/ MAO**	60	30	1684 ± 476	2631.3	5.5

Table S 6 Polymerisation conditions: $\mathrm{Al_{sMAO}}]_0/[\mathrm{Ti}]_0 = 200$, 10 mg catalyst, 2 bar ethylene, 50 mL hexanes, 60 °C, 30 minutes, and $[\mathrm{Al}]_0/[\mathrm{Ti}]_0 = 1000$.

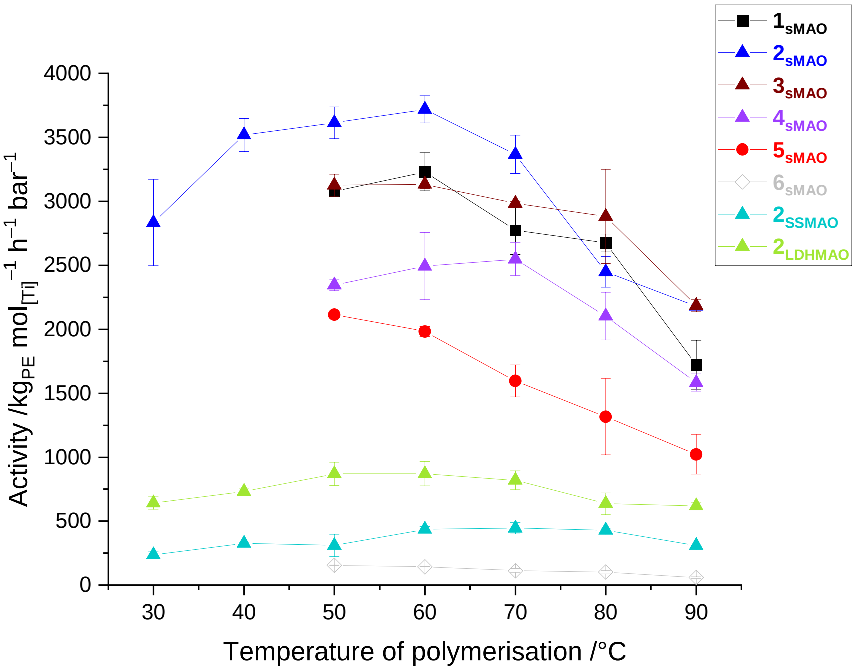

Fig. S 25 Slurry-phase ethylene polymerisation activity as a function of the temperature of polymerisation using sMAO-supported ^{Me_2}SB(^{tBu,Me}ArO,I*)TiCl$_2$ (**1**$_{sMAO}$), ^{Me_2}SB(^{tBu_2}ArO,I*)TiCl$_2$ (**2**$_{sMAO}$), ^{Me_2}SB(^{tBu_2}ArO,I*)TiBr$_2$ (**3**$_{sMAO}$), ^{Me_2}SB(^{tBu_2}ArO,I*)TiI$_2$ (**4**$_{sMAO}$), ^{Me_2}SB($^{(CMe_2Ph)_2}$ArO,I*)TiCl$_2$ (**5**$_{sMAO}$), and ^{Me_2}SB(^{tBu,Me}ArO,Ind)TiCl$_2$ (**6**$_{sMAO}$), and **2** supported on SSMAO (**2**$_{SSMAO}$) and LDHMAO (**2**$_{LDHMAO}$). Polymerisation conditions: 10 mg catalyst, 2 bar ethylene, 50 mL hexanes, 30 minutes, and 150 mg tri-*iso*-butylaluminium. Error bars shown at one standard deviation.

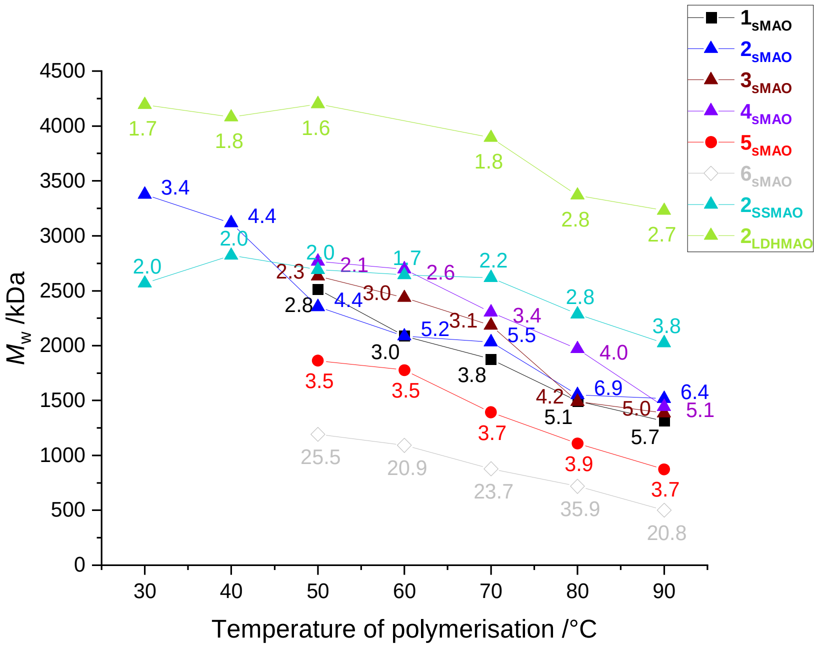

Fig. S 26 Weight-average molecular weight (M_w), with PDIs (M_w/M_n) annotated, of polyethylene synthesised using sMAO-supported ^{Me_2}SB(^{tBu,Me}ArO,I*)TiCl$_2$ (**1**$_{sMAO}$), ^{Me_2}SB(^{tBu_2}ArO,I*)TiCl$_2$ (**2**$_{sMAO}$), ^{Me_2}SB($^{(CMe_2Ph)_2}$ArO,I*)TiCl$_2$ (**5**$_{sMAO}$), and ^{Me_2}SB(^{tBu,Me}ArO,Ind)TiCl$_2$ (**6**$_{sMAO}$), and LDHMAO-supported ^{Me_2}SB(^{tBu_2}ArO,I*)TiCl$_2$ (**2**$_{LDHMAO}$). Polymerisation conditions: 10 mg catalyst, 2 bar ethylene, 50 mL hexanes, 30 minutes, and 150 mg tri-*iso*-butylaluminium.

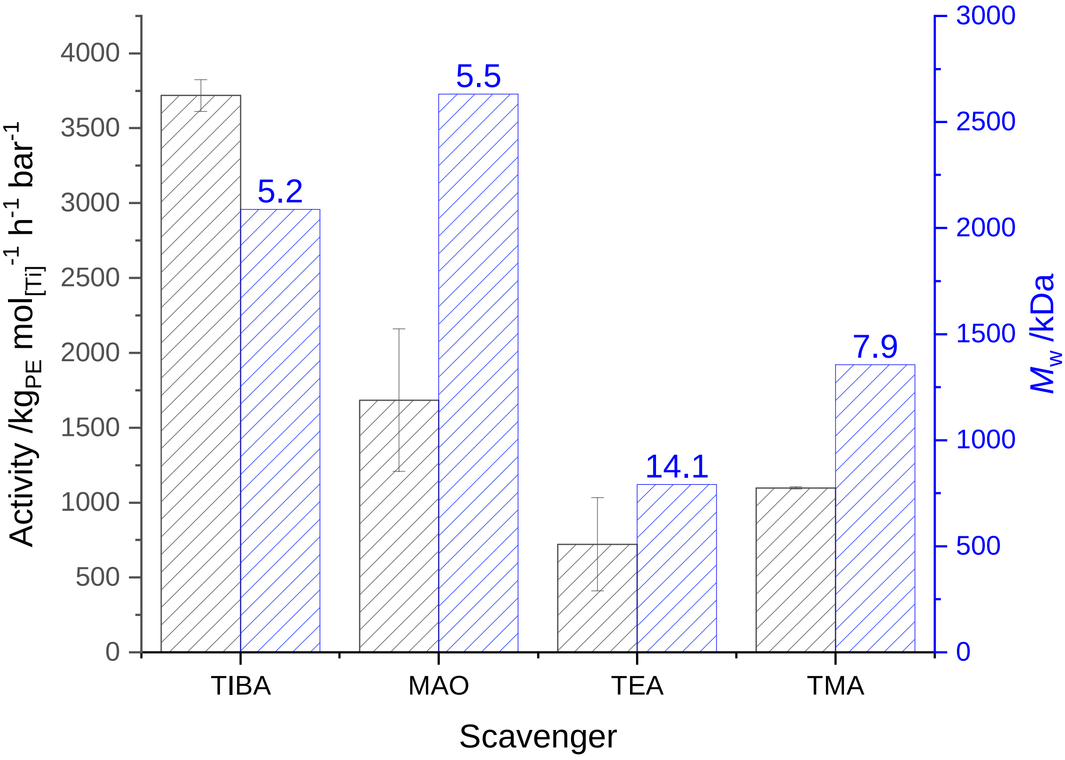

Fig. S 27 Slurry-phase polymerisation activity of, and weight-average molecular weight (with PDIs annotated) of polyethylene produced using ^{Me_2}SB(^{tBu_2}ArO,I*)TiCl$_2$ supported on sMAO (**2_{sMAO}**) with varying aluminium cocatalytic scavengers. Polymerisation conditions: $[Al_{sMAO}]_0/[Ti]_0$ = 200, 10 mg catalyst, 2 bar ethylene, 50 mL hexanes, 60 °C, 30 minutes, and $[Al_{AlR_3}]_0/[Ti]_0$ = 1000. Error bars shown at one standard deviation.

5.3 Gel permeation chromatography

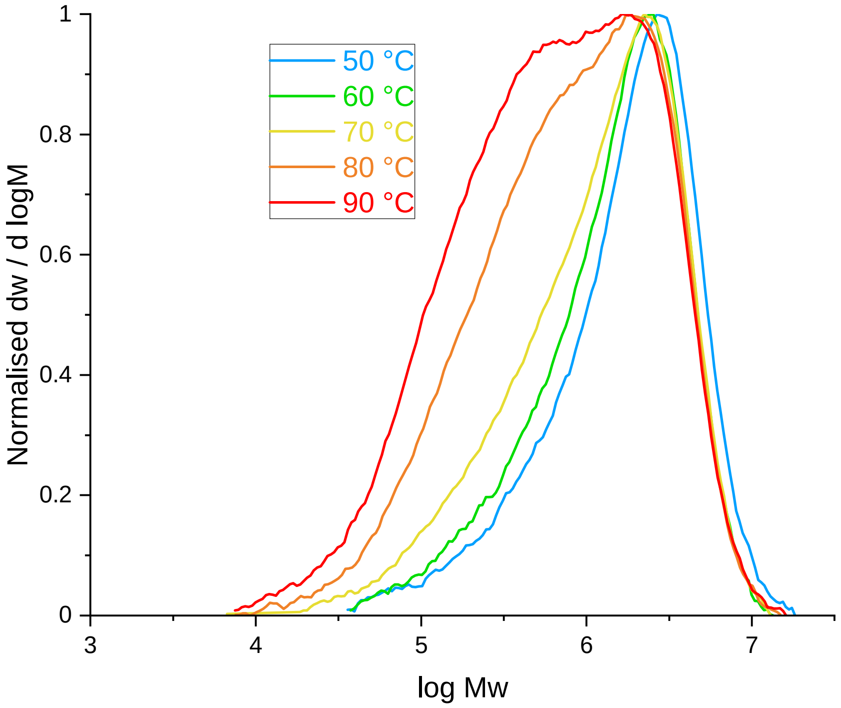

Fig. S 28 Gel permeation chromatograms of PE synthesised by **1**$_{\mathrm{sMAO}}$ as a function of temperature. Polymerisation conditions: 10 mg catalyst, 2 bar ethylene, 50 mL hexanes, 30 minutes, and 150 mg tri-*iso*-butylaluminium.

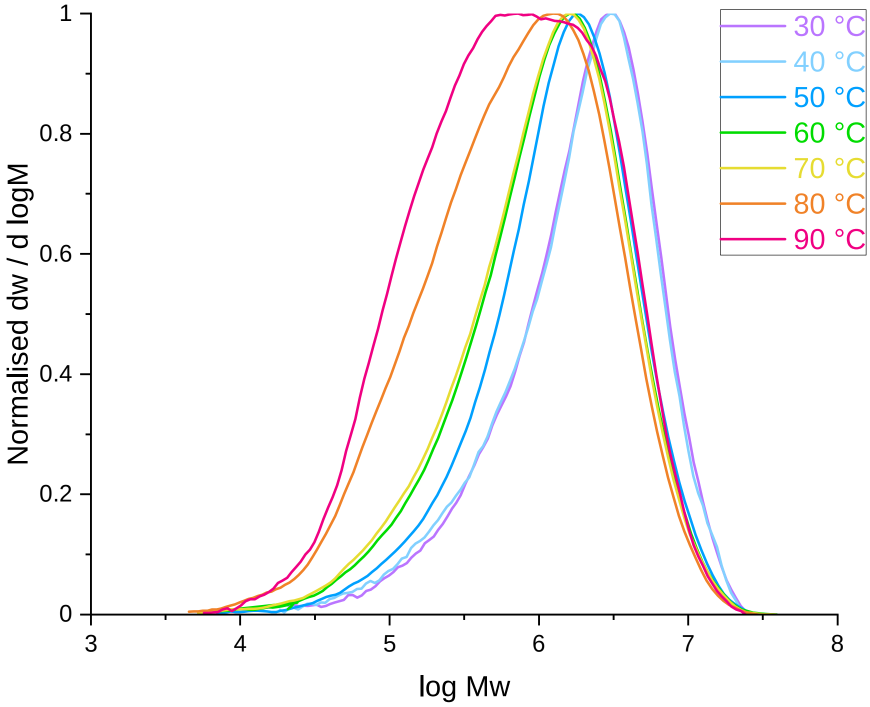

Fig. S 29 Gel permeation chromatograms of PE synthesised by **2**$_{\mathrm{sMAO}}$ as a function of temperature. Polymerisation conditions: 10 mg catalyst, 2 bar ethylene, 50 mL hexanes, 30 minutes, and 150 mg tri-*iso*-butylaluminium.

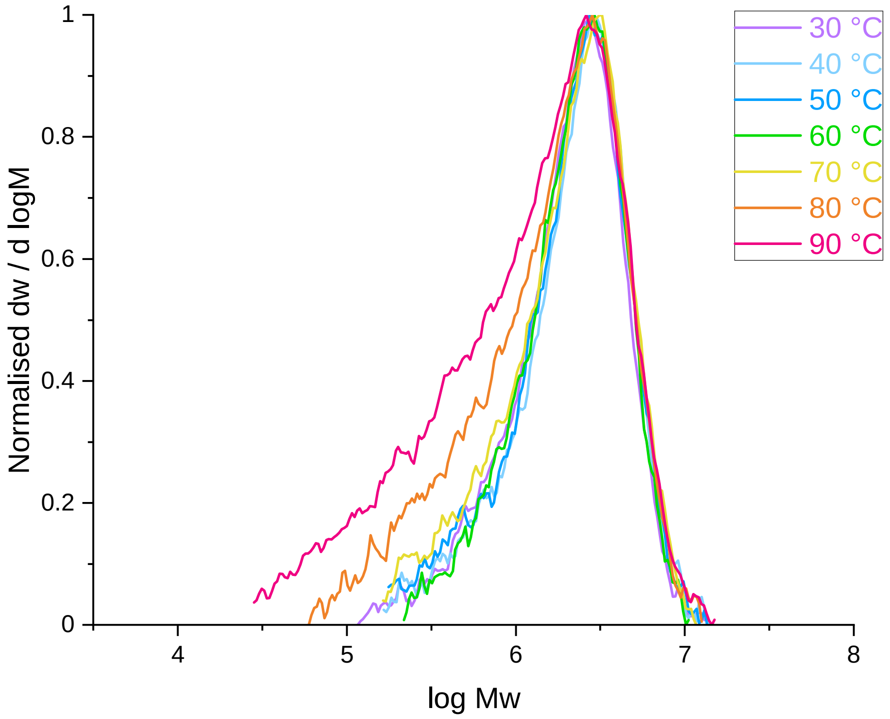

Fig. S 30 Gel permeation chromatograms of PE synthesised by $\mathbf{2}_{\mathrm{SSMAO}}$ as a function of temperature. Polymerisation conditions: 10 mg catalyst, 2 bar ethylene, 50 mL hexanes, 30 minutes, and 150 mg tri-*iso*-butylaluminium.

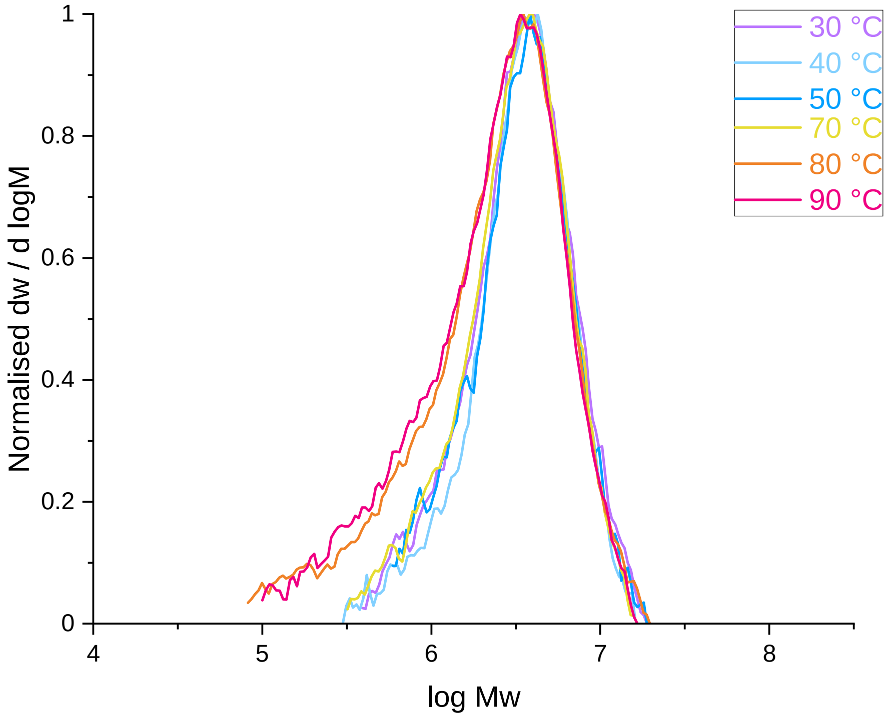

Fig. S 31 Gel permeation chromatograms of PE synthesised by $\mathbf{2}_{\mathrm{LDHMAO}}$ as a function of temperature. Polymerisation conditions: 10 mg catalyst, 2 bar ethylene, 50 mL hexanes, 30 minutes, and 150 mg tri-*iso*-butylaluminium.

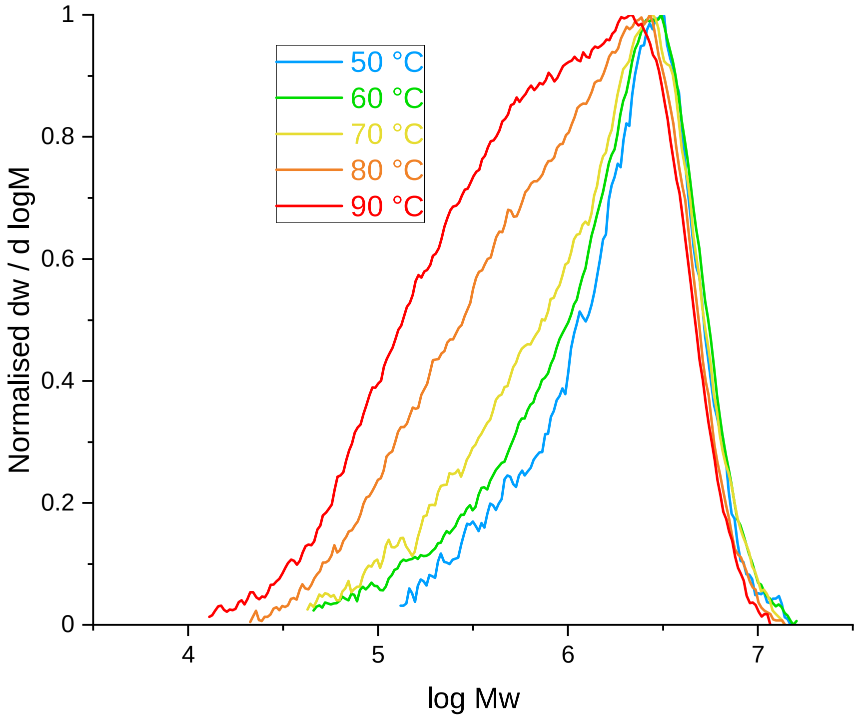

Fig. S 32 Gel permeation chromatograms of PE synthesised by **3**$_{\mathbf{sMAO}}$ as a function of temperature. Polymerisation conditions: 10 mg catalyst, 2 bar ethylene, 50 mL hexanes, 30 minutes, and 150 mg tri-*iso*-butylaluminium.

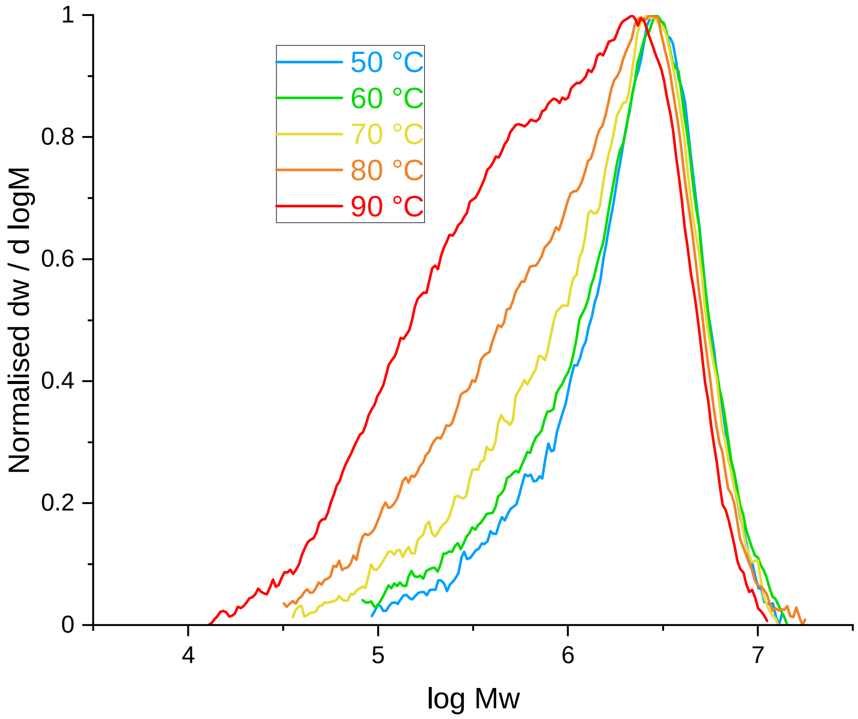

Fig. S 33 Gel permeation chromatograms of PE synthesised by **4**$_{\mathbf{sMAO}}$ as a function of temperature. Polymerisation conditions: 10 mg catalyst, 2 bar ethylene, 50 mL hexanes, 30 minutes, and 150 mg tri-*iso*-butylaluminium.

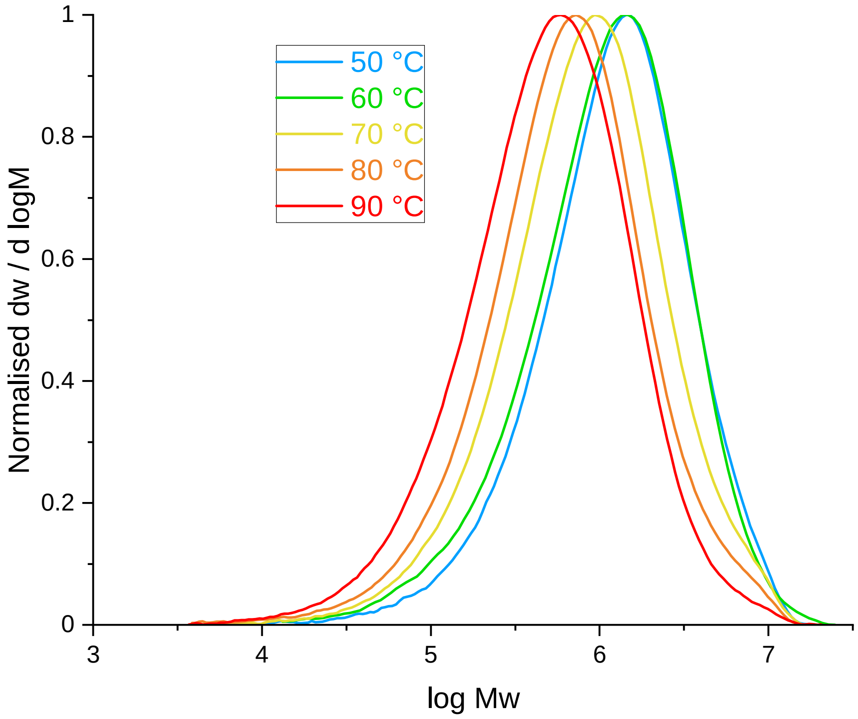

Fig. S 34 Gel permeation chromatograms of PE synthesised by **5**$_{\mathbf{sMAO}}$ as a function of temperature. Polymerisation conditions: 10 mg catalyst, 2 bar ethylene, 50 mL hexanes, 30 minutes, and 150 mg tri-*iso*-butylaluminium.

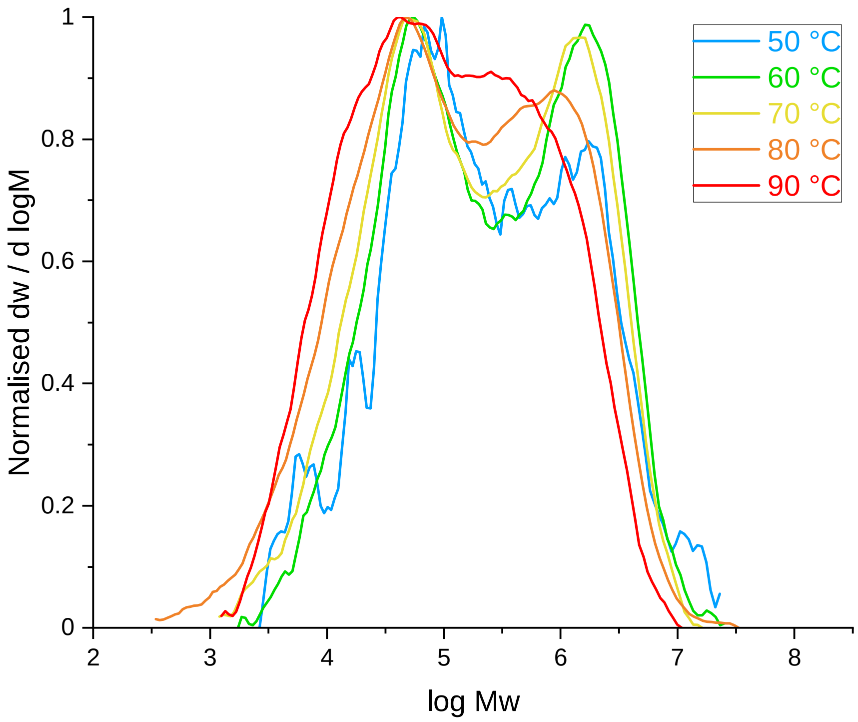

Fig. S 35 Gel permeation chromatograms of PE synthesised by **6**$_{\mathbf{sMAO}}$ as a function of temperature. Polymerisation conditions: 10 mg catalyst, 2 bar ethylene, 50 mL hexanes, 30 minutes, and 150 mg tri-*iso*-butylaluminium.

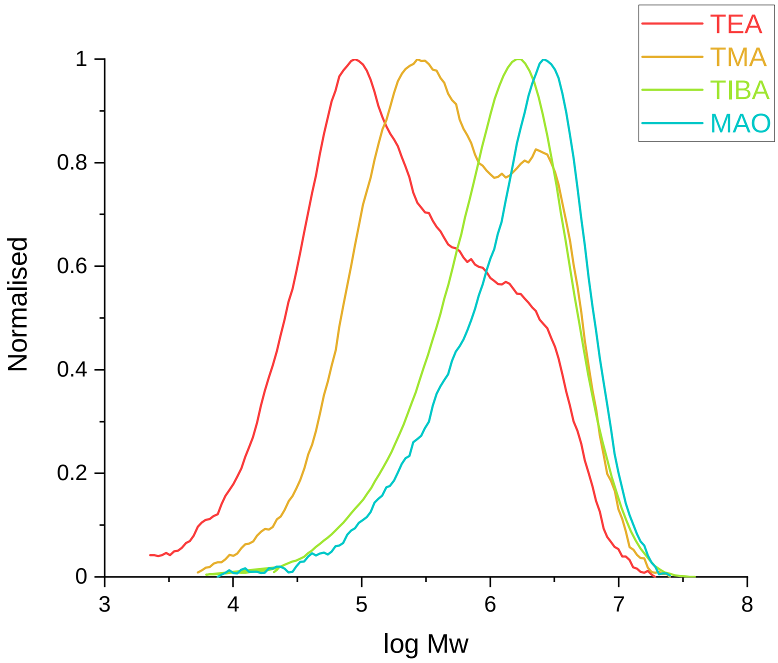

Fig. S 36 Gel permeation chromatograms of PE synthesised by $\mathbf{2}_{\mathbf{sMAO}}$ with varying aluminium cocatalytic scavengers. Polymerisation conditions: $[Al_{sMAO}]_0/[Ti]_0$ = 200, 10 mg catalyst, 2 bar ethylene, 50 mL hexanes, 60 °C, 30 minutes, and $[Al_{AlR_3}]_0/[Ti]_0$ = 1000.

5.4 Scanning Electron Microscopy images

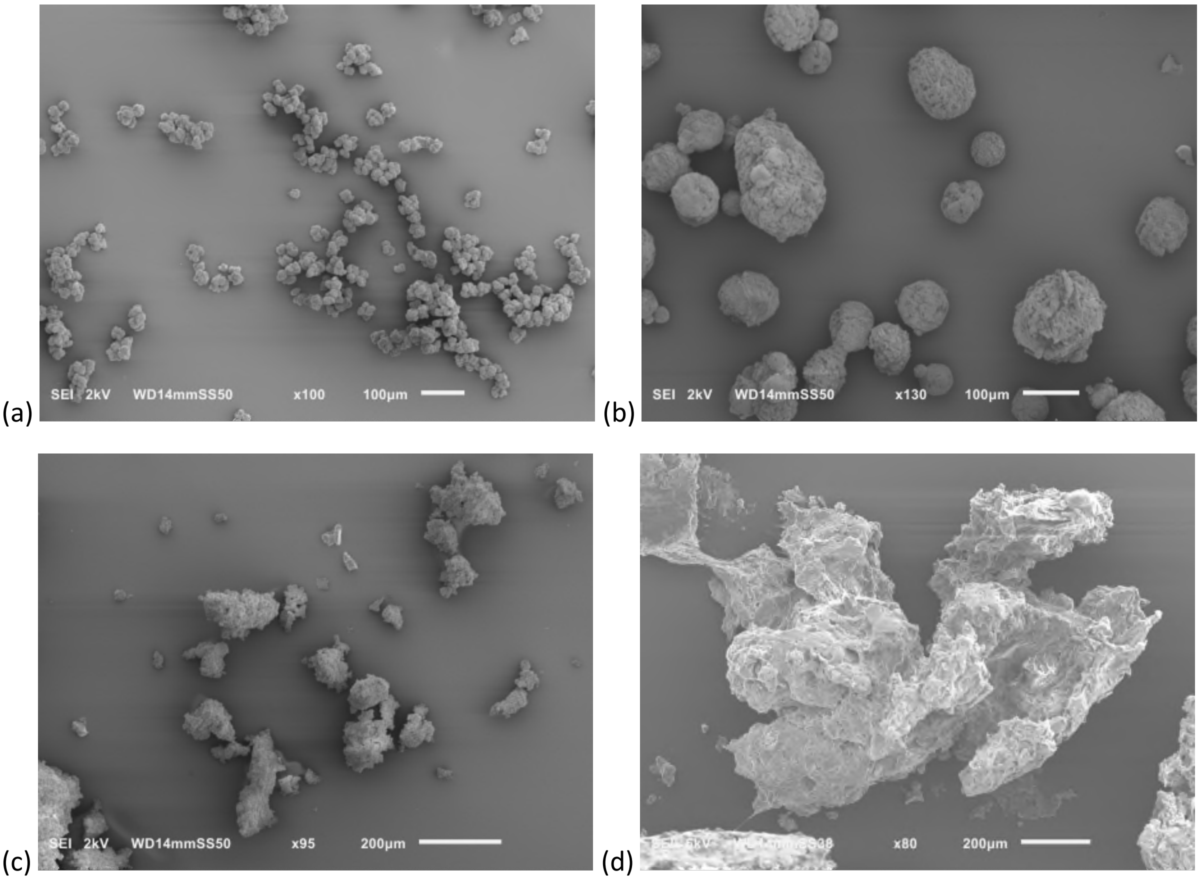

Fig. S 37 Scanning electron micrographs of polyethylene, synthesised using (a) $\mathbf{2_{sMAO}}$, (b) $\mathbf{2_{SSMAO}}$, (c) $\mathbf{2_{LDHMAO}}$, and (d) solution-phase **2**. Slurry-phase polymerisation conditions: $[\mathrm{Al_{support}}]_0/[\mathrm{Ti}]_0 = 200$, 150 mg TIBA, 2 bar ethylene, 10 mg catalyst, 50 mL hexanes, 60 °C, and 30 minutes. Solution-phase polymerisation conditions: $[\mathrm{Al_{MAO}}]_0/[\mathrm{Ti}]_0 = 1000$, 2 bar ethylene, 414 µg catalyst, 49 mL hexanes, 1 mL toluene, 60 °C, and 5 minutes.

5.5 Differential Scanning Calorimetry

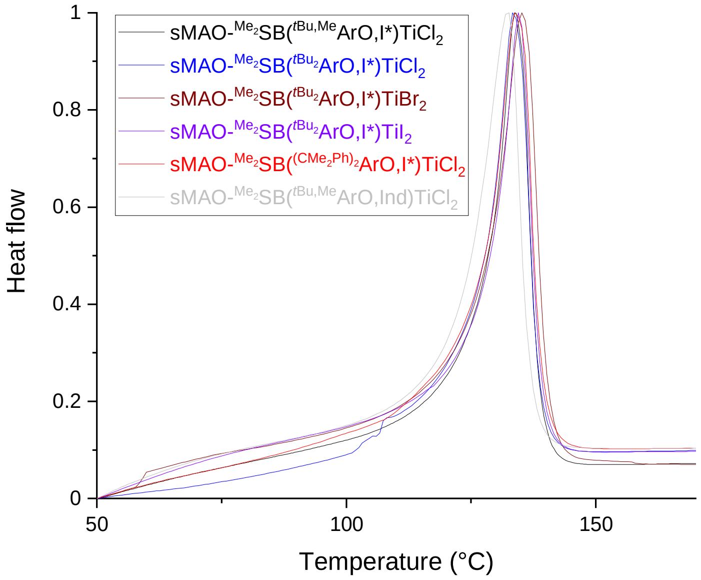

Fig. S 38 Differential scanning calorimetry plots (heating at 20 K min^{-1}, second melting endotherm shown), normalised for clarity, of PE produced by **1**$_{\text{sMAO}}$, **2**$_{\text{sMAO}}$, **3**$_{\text{sMAO}}$, **4**$_{\text{sMAO}}$, **5**$_{\text{sMAO}}$, and **6**$_{\text{sMAO}}$. Polymerisation conditions: $[\text{Al}_{\text{sMAO}}]_0/[\text{Ti}]_0 = 200$, 150 mg TIBA, 2 bar ethylene, 10 mg catalyst, 50 mL hexanes, 60 °C, and 30 minutes.

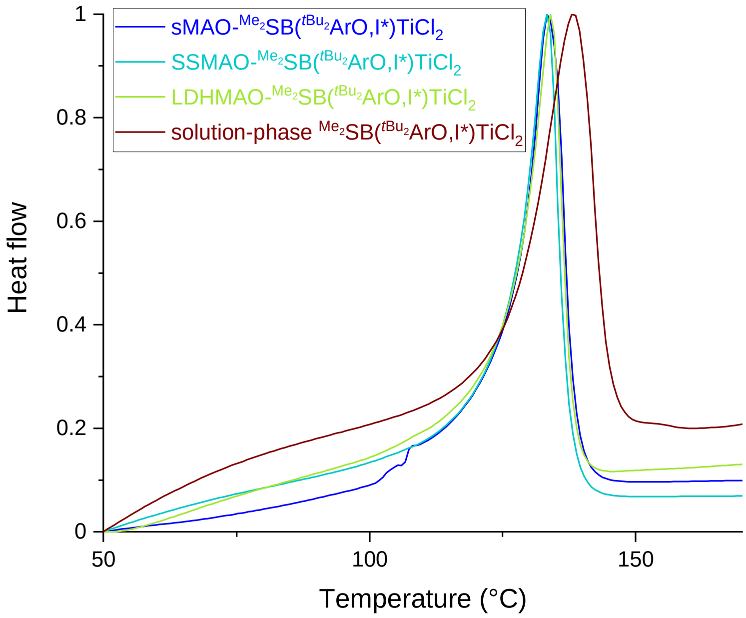

Fig. S 39 Differential scanning calorimetry plots (heating at 20 K min^{-1}, second melting endotherm shown), normalised for clarity, of PE produced by **2**$_{\text{sMAO}}$, **2**$_{\text{SSMAO}}$, **2**$_{\text{LDHMAO}}$, and solution-phase **2**. Slurry-phase polymerisation conditions: $[\text{Al}_{\text{support}}]_0/[\text{Ti}]_0 = 200$, 150 mg TIBA, 2 bar ethylene, 10 mg catalyst, 50 mL hexanes, 60 °C, and 30 minutes. Solution-phase polymerisation conditions: $[\text{Al}_{\text{MAO}}]_0/[\text{Ti}]_0 = 1000$, 2 bar ethylene, 414 µg catalyst, 49 mL hexanes, 1 mL toluene, 60 °C, and 5 minutes.

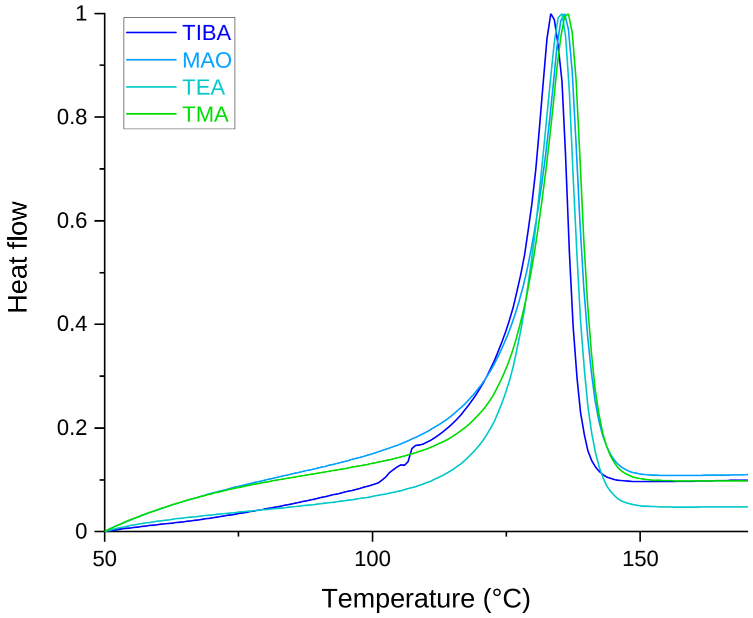

Fig. S 40 Differential scanning calorimetry plots (heating at 20 K min^{-1}, second melting endotherm shown), normalised for clarity, of PE produced by $\mathbf{2}_{\mathbf{sMAO}}$. Polymerisation conditions: $[Al_{sMAO}]_0/[Ti]_0$ = 200, 10 mg catalyst, 2 bar ethylene, 50 mL hexanes, 60 °C, 30 minutes, and $[Al]_0/[Ti]_0$ = 1000.

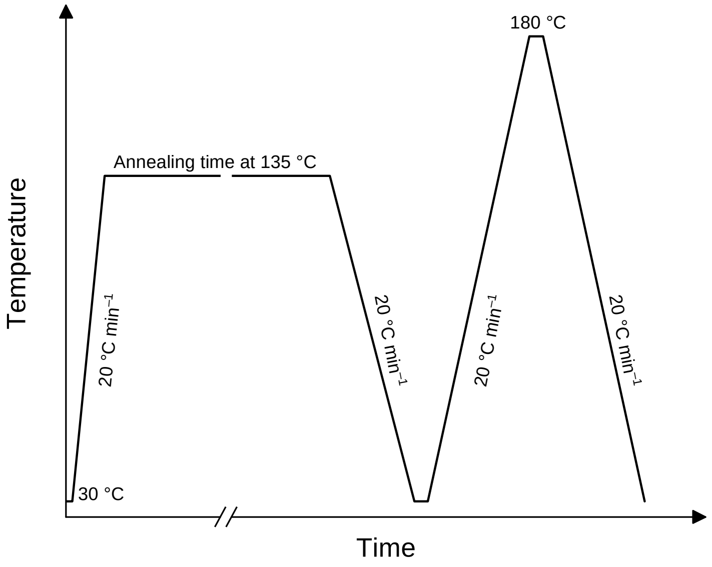

Fig. S 41 Graphical representation of the protocol used for DSC annealing experiments.[13]

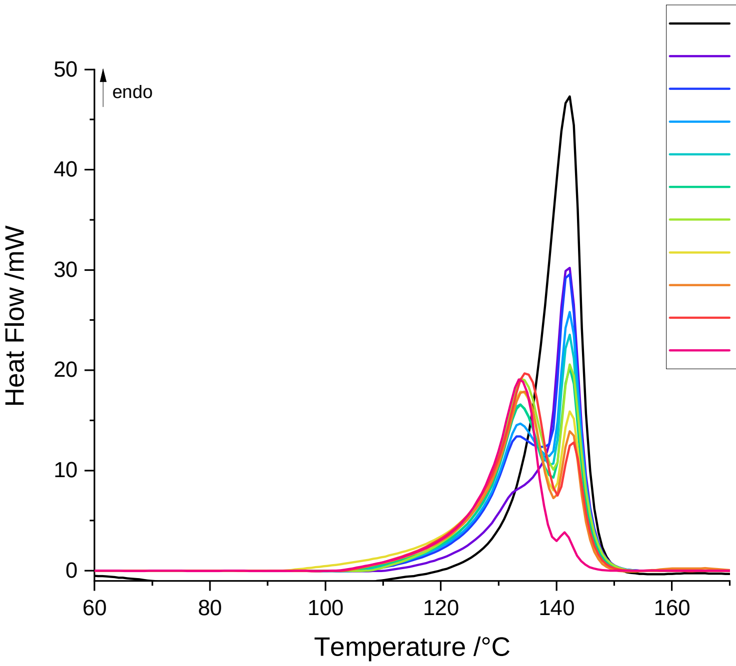

Fig. S 42 Heating cycle of UHMWPE after annealing at 135 °C for different annealing times. Synthesis conditions: **2_{sMAO}**, T_p = 30°C, $[Al_{sMAO}]_0/[Ti]_0$ = 200, 10 mg catalyst, 150 mg TIBA, 2 bar ethylene, 50 mL hexanes, and 30 minutes. M_w = 3376.0 kDa, PDI = 3.4.

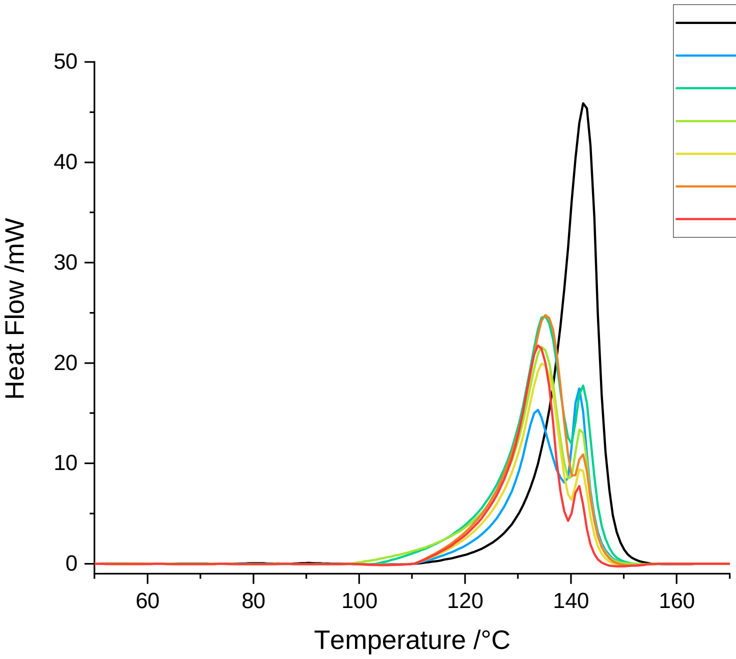

Fig. S 43 Heating cycle of UHMWPE after annealing at 135 °C for different annealing times. Synthesis conditions: **2_{sMAO}**, T_p = 60°C, $[Al_{sMAO}]_0/[Ti]_0$ = 200, 10 mg catalyst, 150 mg TIBA, 2 bar ethylene, 50 mL hexanes, and 30 minutes. M_w = 2087.5 kDa, PDI = 5.2.

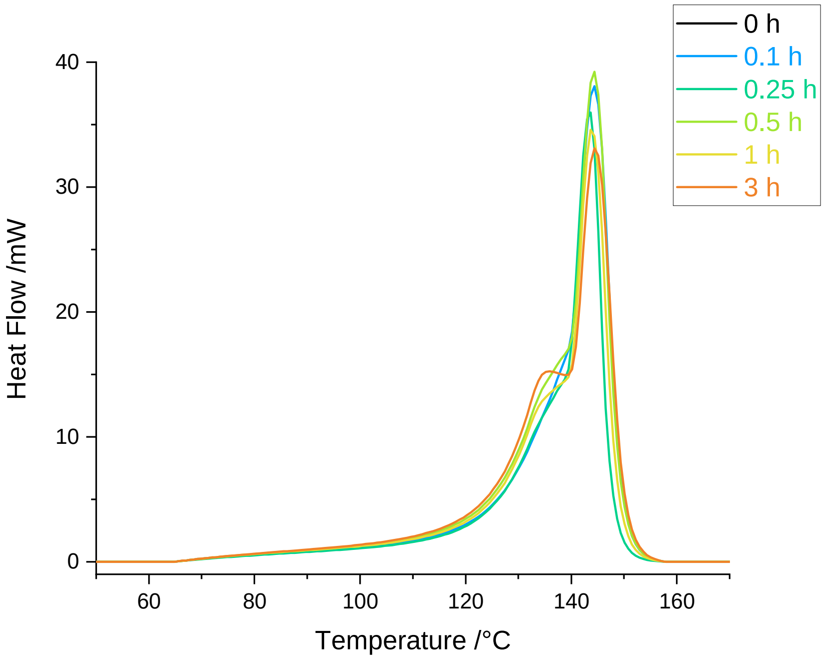

Fig. S 44 Heating cycle of UHMWPE after annealing at 135 °C for different annealing times. Synthesis conditions: $\mathbf{3}_{\mathbf{sMAO}}$, T_p = 60°C, $[Al_{sMAO}]_0/[Ti]_0$ = 200, 10 mg catalyst, 150 mg TIBA, 2 bar ethylene, 50 mL hexanes, and 30 minutes. M_w = 2437.7 kDa, PDI = 3.0.

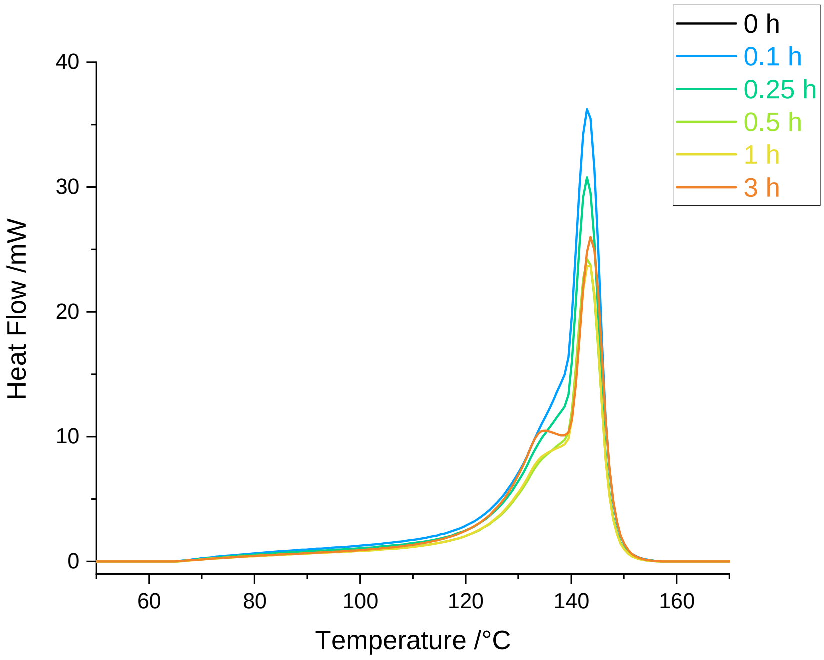

Fig. S 45 Heating cycle of UHMWPE after annealing at 135 °C for different annealing times. Synthesis conditions: $\mathbf{4}_{\mathbf{sMAO}}$, T_p = 60°C, $[Al_{sMAO}]_0/[Ti]_0$ = 200, 10 mg catalyst, 150 mg TIBA, 2 bar ethylene, 50 mL hexanes, and 30 minutes. M_w = 2696.2 kDa, PDI = 2.6.

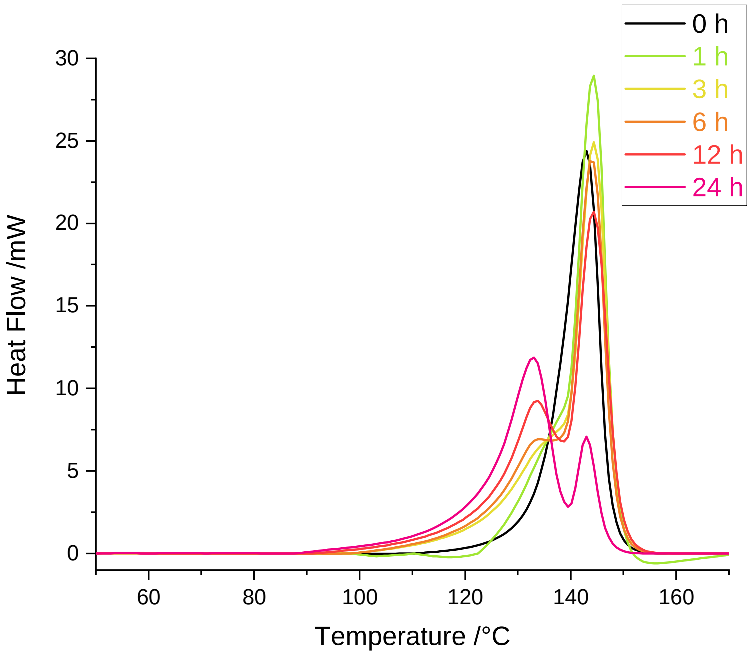

Fig. S 46 Heating cycle of UHMWPE after annealing at 135 °C for different annealing times. Synthesis conditions: **2**$_{\mathbf{LDHMAO}}$, T_p = 30°C, [Al_{MAO}]$_0$/[Ti]$_0$ = 200, 10 mg catalyst, 150 mg TIBA, 2 bar ethylene, 50 mL hexanes, and 30 minutes. M_w = 4195.0 kDa, PDI = 1.7.

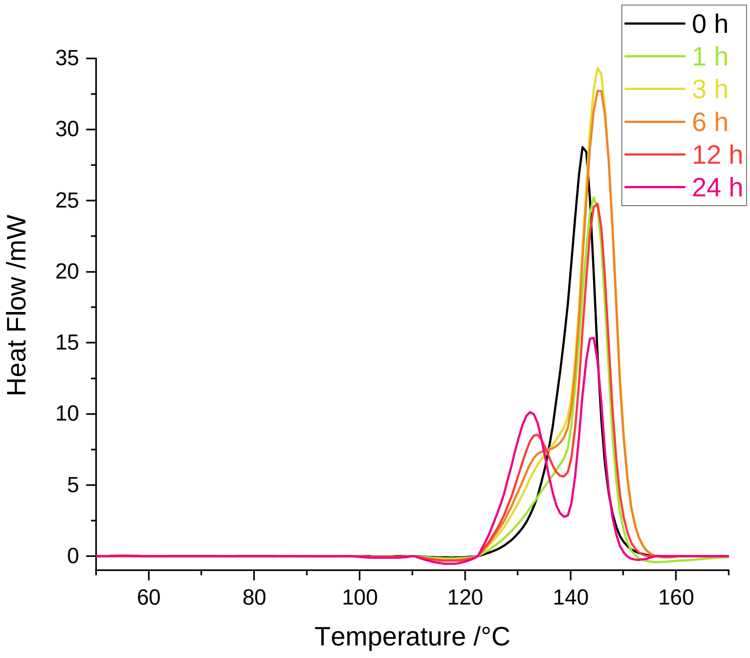

Fig. S 47 Heating cycle of UHMWPE after annealing at 135 °C for different annealing times. Synthesis conditions: **2**$_{\mathbf{LDHMAO}}$, T_p = 60°C, [Al_{MAO}]$_0$/[Ti]$_0$ = 200, 10 mg catalyst, 150 mg TIBA, 2 bar ethylene, 50 mL hexanes, and 30 minutes.

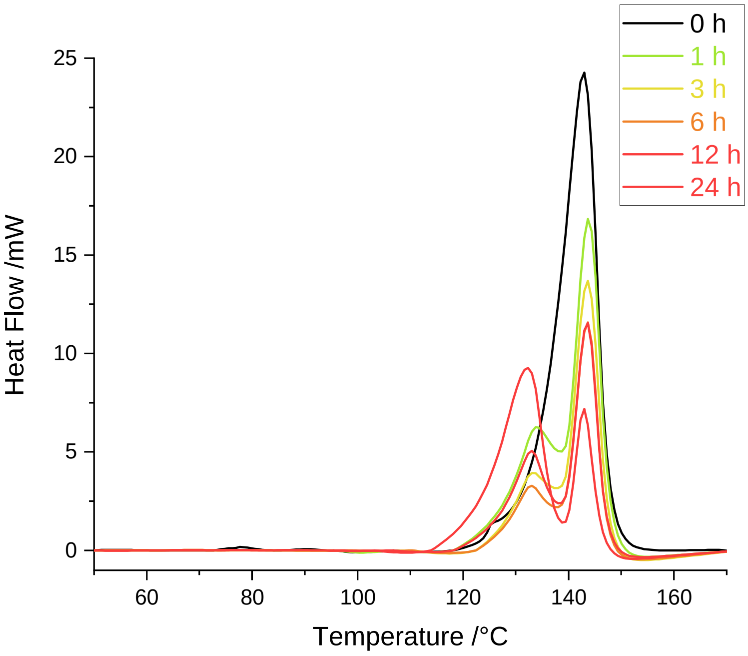

Fig. S 48 Heating cycle of UHMWPE after annealing at 135 °C for different annealing times. Synthesis conditions: **2**$_{\mathbf{LDHMAO}}$, T_p = 90°C, $[Al_{MAO}]_0/[Ti]_0$ = 200, 10 mg catalyst, 150 mg TIBA, 2 bar ethylene, 50 mL hexanes, and 30 minutes. M_w = 3230.0 kDa, PDI = 2.7.

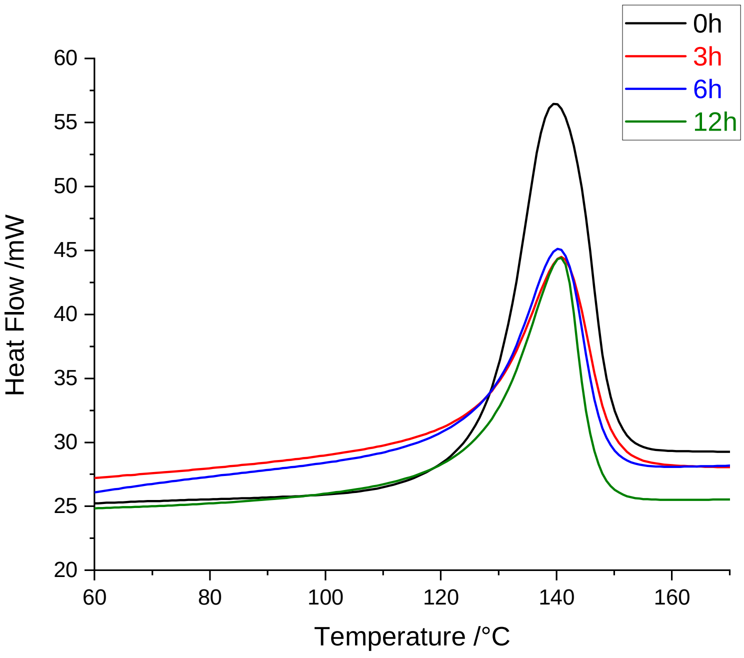

Fig. S 49 Heating cycle of UHMWPE after annealing at 135 °C for different annealing times. Synthesis conditions: **2**, T_p = 30°C, $[Al_{MAO}]_0/[Ti]_0$ = 1000, 2 bar ethylene, 414 µg catalyst, 49 mL hexanes, 1 mL toluene, and 5 minutes.

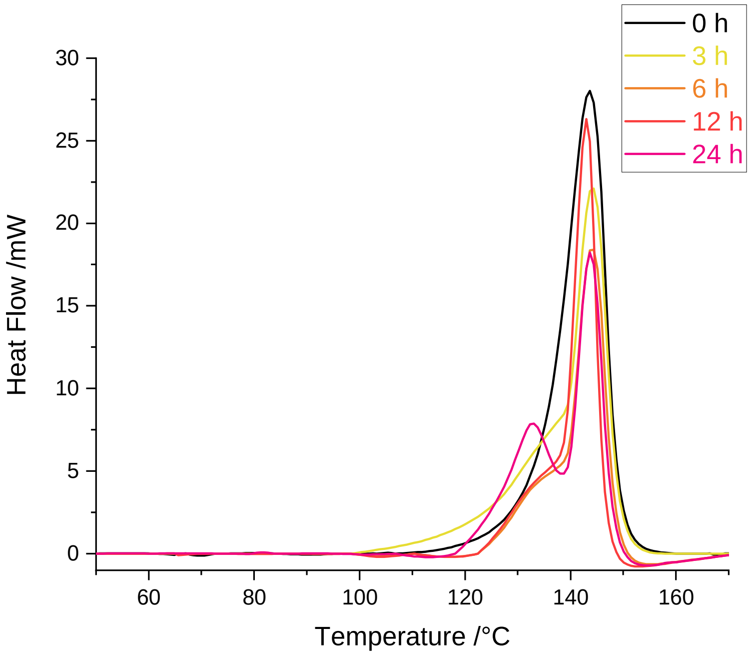

Fig. S 50 Heating cycle of UHMWPE after annealing at 135 °C for different annealing times. Synthesis conditions: **2**$_{\mathbf{SSMAO}}$, T_p = 30°C, $[Al_{MAO}]_0/[Ti]_0$ = 200, 10 mg catalyst, 150 mg TIBA, 2 bar ethylene, 50 mL hexanes, and 30 minutes. M_w = 2567.9 kDa, PDI = 2.0.

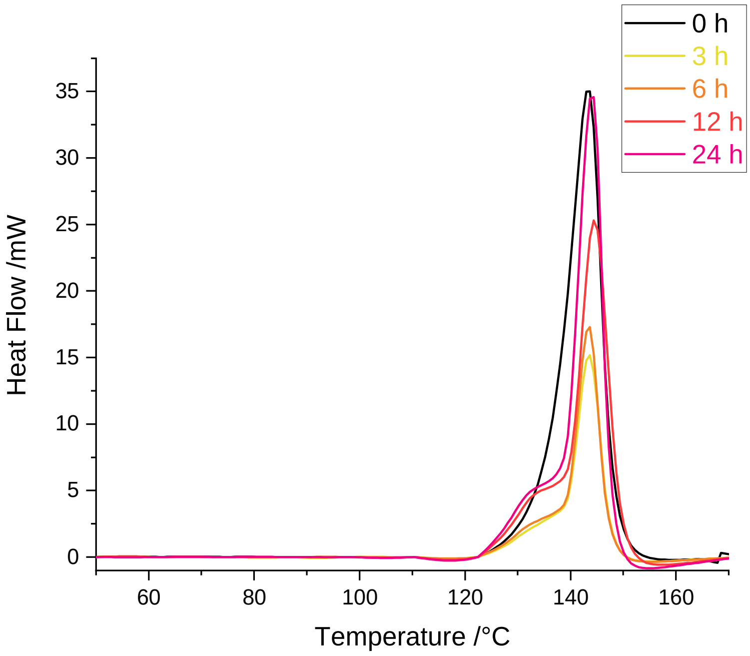

Fig. S 51 Heating cycle of UHMWPE after annealing at 135 °C for different annealing times. Synthesis conditions: **2**$_{\mathbf{SSMAO}}$, T_p = 60°C, $[Al_{MAO}]_0/[Ti]_0$ = 200, 10 mg catalyst, 150 mg TIBA, 2 bar ethylene, 50 mL hexanes, and 30 minutes. M_w = 2643.8 kDa, PDI = 1.7.

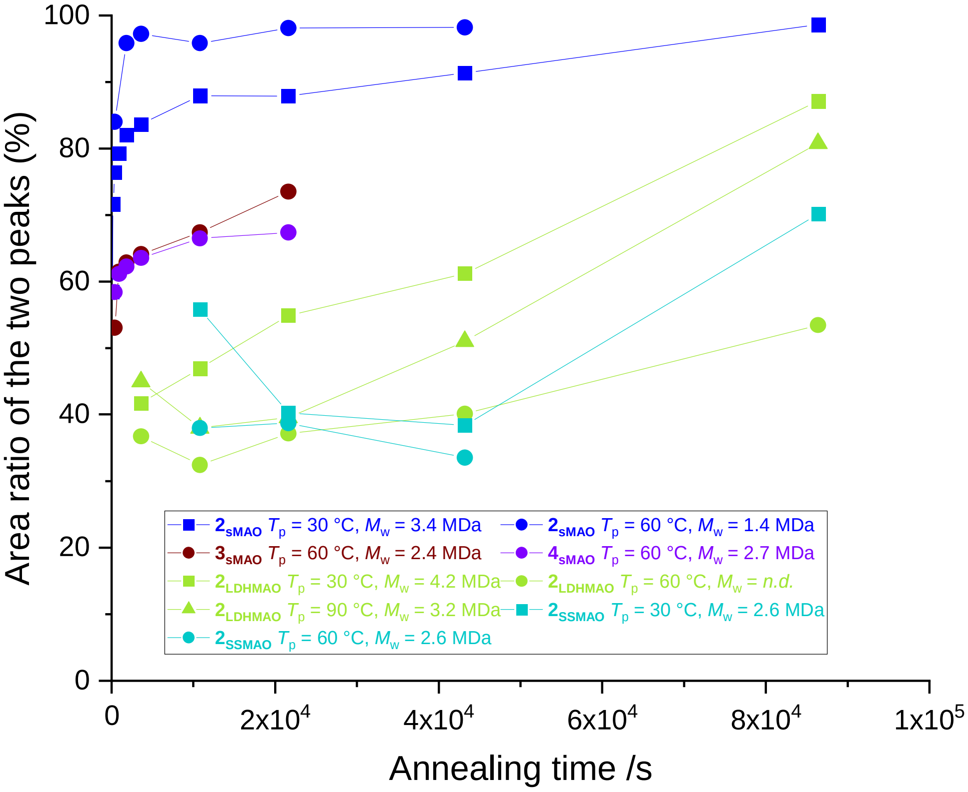

Fig. S 52 Evolution of the normalised area of the DSC peaks as a function of annealing time.

5.6 Solid-state NMR spectroscopy

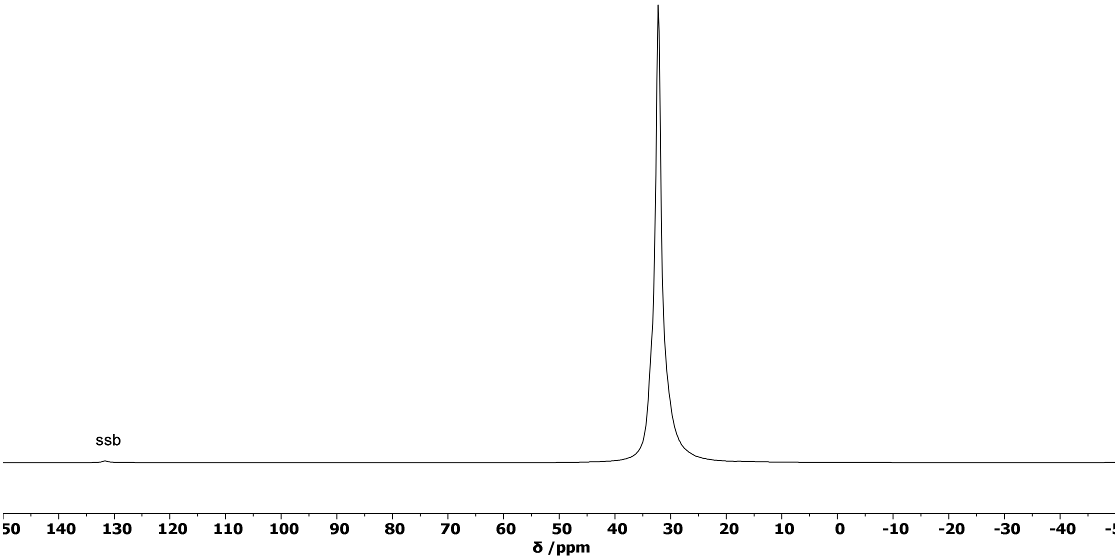

Fig. S 53 ^{13}C CPMAS ssNMR spectrum (10 kHz, 101 MHz, 298 K) of polyethylene synthesised using $\mathbf{1}_{\text{sMAO}}$. Polymerisation conditions: 10 mg catalyst, 2 bar ethylene, 50 mL hexanes, 150 mg TIBA, 30 minutes, and 60 °C. Spinning side band denoted ssb.

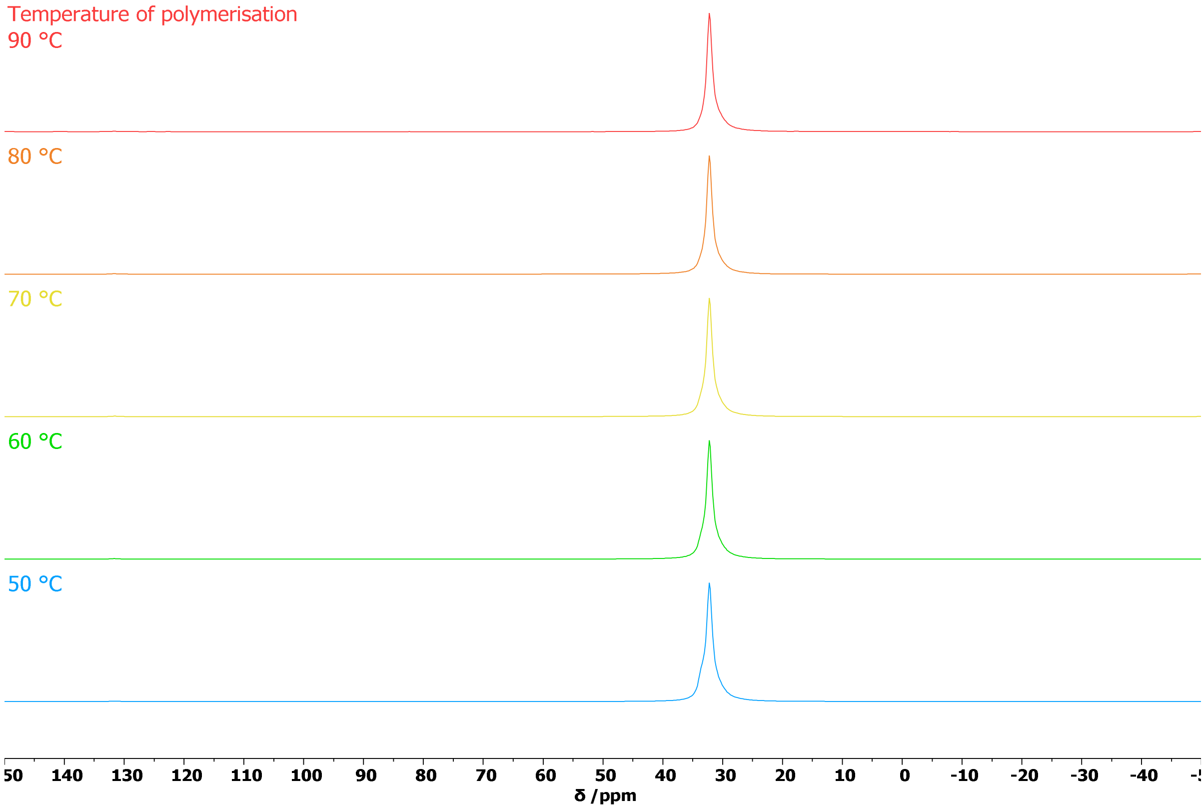

Fig. S 54 ^{13}C CPMAS ssNMR spectrum (10 kHz, 101 MHz, 298 K) of polyethylene synthesised using $\mathbf{2}_{\mathrm{sMAO}}$ across a temperature of polymerisation of 50–90 °C. Polymerisation conditions: 10 mg catalyst, 2 bar ethylene, 50 mL hexanes, 150 mg TIBA, and 30 minutes.

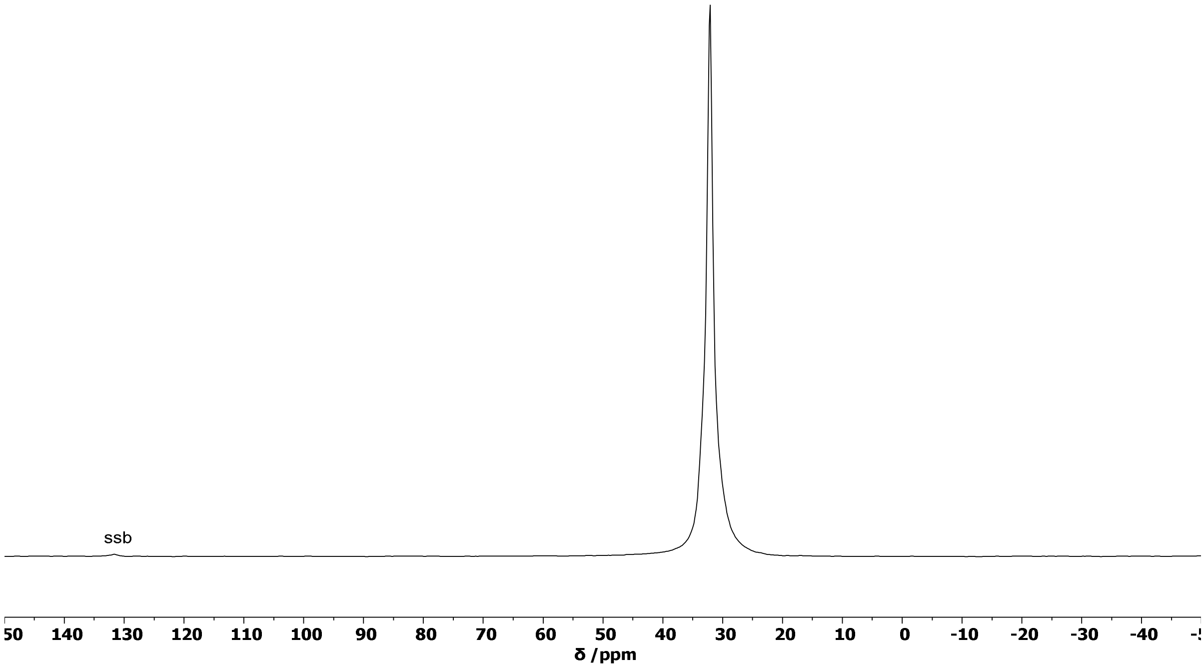

Fig. S 55 ^{13}C CPMAS ssNMR spectrum (10 kHz, 101 MHz, 298 K) of polyethylene synthesised using $\mathbf{5}_{\mathrm{sMAO}}$. Polymerisation conditions: 10 mg catalyst, 2 bar ethylene, 50 mL hexanes, 150 mg TIBA, 30 minutes, and 60 °C. Spinning side band denoted ssb.

5.7 Infrared (FTIR) spectroscopy

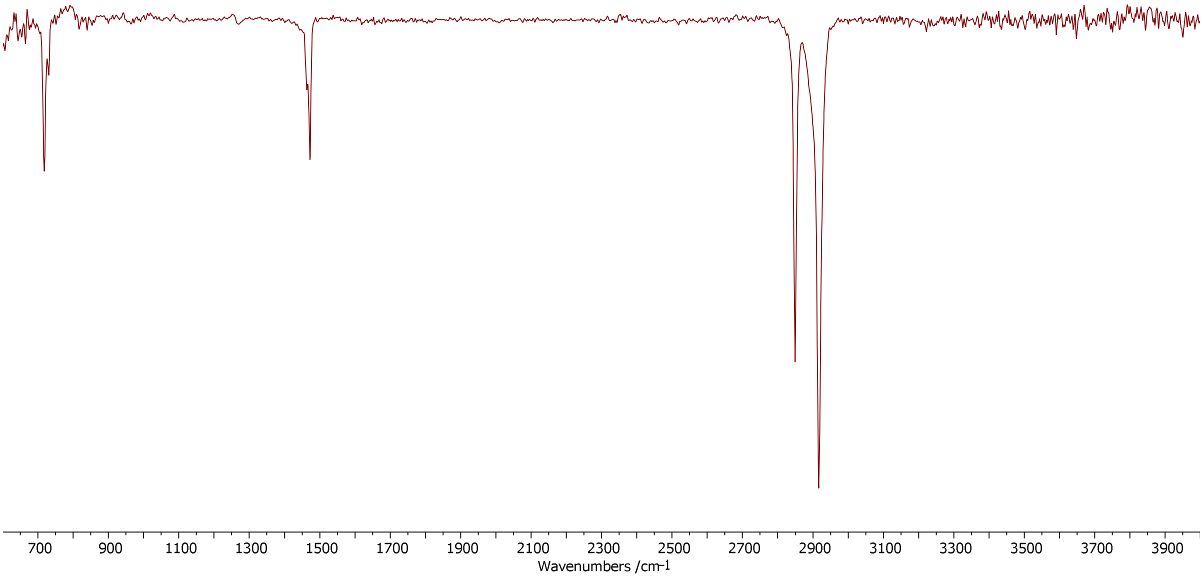

Fig. S 56 FTIR spectrum of polyethylene synthesised using $\mathbf{2}_{\mathrm{sMAO}}$. Polymerisation conditions: 10 mg catalyst, 2 bar ethylene, 50 mL hexanes, 150 mg TIBA, 30 minutes, and 60 °C.

6. References

1 D. F. Shriver and M. A. Drezdon, *The Manipulation of Air-Sensitive Compounds*, 2 edn., Wiley, 1986.
2 J. Cosier and A. M. Glazer, *J. Appl. Crystallogr.*, 1986, **19**, 105-107.
3 U. K. L. Oxford Diffraction Agilent Technologies, Yarnton, England.
4 A. Altomare, G. Cascarano, C. Giacovazzo, A. Guagliardi, *J. Appl. Crystallogr.*, 1993, **26**, 343-350.
5 L. Palatinus and G. Chapuis, *J. Appl. Crystallogr.*, 2007, **40**, 786-790.
6 L. Farrugia, *J. Appl. Crystallogr.*, 1999, **32**, 837-838.
7 A. L. Spek, *J. Appl. Crystallogr.*, 2003, **36**, 7-13.
8 L. J. Farrugia, *J. Appl. Crystallogr.*, 2012, **45**, 849-854.
9 C. Görl, E. Betthausen, H. G. Alt, *Polyhedron*, 2016, **118**, 37-51.
10 H. Hanaoka, T. Hino, H. Souda, K. Yanagi, Y. Oda, A. Imai, *J. Organomet. Chem.*, 2007, **692**, 4059-4066.
11 G. E. Hickman, C. M. R. Wright, A. F. R. Kilpatrick, Z. R. Turner, J.-C. Buffet, D. O'Hare, *Mol. Catal.*, 2019, **468**, 139-147.
12 C. P. Chen, M. S. Yang, Q. Wang, J. C. Buffet, D. O'Hare, *Journal of Materials Chemistry A*, 2014, **2**, 15102-15110.
13 D. Romano, N. Tops, E. Andablo-Reyes, S. Ronca, S. Rastogi, *Macromol.*, 2014, **47**, 4750-4760.